cmgh
CELLULAR AND MOLECULAR GASTROENTEROLOGY AND HEPATOLOGY

ORIGINAL RESEARCH

STIM1 Deficiency In Intestinal Epithelium Attenuates Colonic Inflammation and Tumorigenesis by Reducing ER Stress of Goblet Cells

Xiaojing Liang,[1,*] Jiansheng Xie,[1,*] Hao Liu,[1] Rongjie Zhao,[1] Wei Zhang,[1] Haidong Wang,[1] Hongming Pan,[1] Yubin Zhou,[2] and Weidong Han[1]

[1]*Department of Medical Oncology, Sir Run Run Shaw Hospital, College of Medicine, Zhejiang University, Hangzhou, Zhejiang, People's Republic of China;* [2]*Center for Translational Cancer Research, Institute of Biosciences and Technology, Texas A&M University Health Science Center, Houston, Texas*

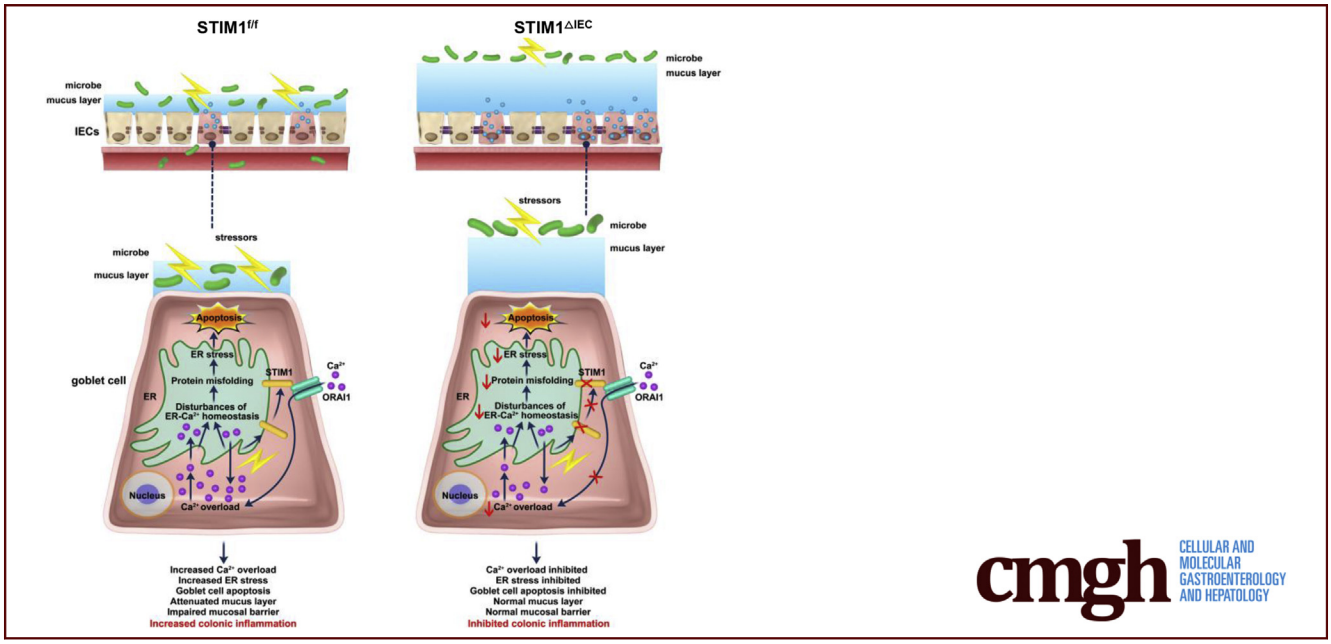

SUMMARY

Stromal interaction molecule 1 deficiency in intestinal epithelium reduces goblet cell endoplasmic reticulum stress and subsequent cell loss induced by stressors through attenuating Ca^{2+} overload, maintaining the mucus layer, and decreasing microbial exposure, therefore, rendering intestinal epithelium-specific stromal interaction molecule 1 conditional knockout mice less susceptible to colitis and colitis-associated colorectal cancer.

BACKGROUND & AIMS: As an indispensable component of store-operated Ca^{2+} entry, stromal interaction molecule 1 (STIM1) is known to promote colorectal cancer and T-cell–mediated inflammatory diseases. However, whether the intestinal mucosal STIM1 is involved in inflammatory bowel diseases (IBDs) is unclear. This study aimed to investigate the role of intestinal epithelial STIM1 in IBD.

METHODS: Inflammatory and matched normal intestinal tissues were collected from IBD patients to investigate the expression of STIM1. Intestinal epithelium-specific STIM1 conditional knockout mice ($STIM1^{\Delta IEC}$) were generated and induced to develop colitis and colitis-associated colorectal cancer. The mucosal barrier, including the epithelial barrier and mucus barrier, was analyzed. The mechanisms by which STIM1 regulate goblet cell endoplasmic reticulum stress and apoptosis were assessed.

RESULTS: STIM1 could regulate intestinal epithelial homeostasis. STIM1 was augmented in the inflammatory intestinal tissues of IBD patients. In dextran sodium sulfate–induced colitis, STIM1 deficiency in intestinal epithelium reduced the loss of goblet cells through alleviating endoplasmic reticulum stress induced by disturbed Ca^{2+} homeostasis, resulting in the maintenance of the integrated mucus layer. These effects prevented commensal bacteria from contacting and stimulating the intestinal epithelium of $STIM1^{\Delta IEC}$ mice and thereby rendered $STIM1^{\Delta IEC}$ mice less susceptible to colitis and colitis-associated colorectal cancer. In addition, microbial diversity in dextran

sodium sulfate–treated STIM1$^{\Delta IEC}$ mice slightly shifted to an advantageous bacteria, which further protected the intestinal epithelium.

CONCLUSIONS: Our results establish STIM1 as a crucial regulator for the maintenance of the intestinal barrier during colitis and provide a potential target for IBD treatment. *(Cell Mol Gastroenterol Hepatol 2022;14:193–217; https://doi.org/10.1016/j.jcmgh.2022.03.007)*

Keywords: IBD; Mucosal Barrier; Goblet Cells; ER Stress.

Under normal conditions, the intestinal tract is filled with kilograms of microbes, and the luminal commensal bacteria is separated from the intestinal mucosa, especially from the lamina propria, which is involved in innate and adaptive immune responses to defend against commensal bacteria.[1] The complete separation of commensal bacteria from intestinal epithelium is mainly dependent on the mucosal barrier provided by intestinal epithelial cells (IECs), including a monolayer epithelial barrier and an extracellular mucus barrier. The epithelial barrier is formed by IECs that are arranged in a single layer with apical junctional complexes, including tight junctions and adherens junctions, that constitute strong adhesive bonds to seal the paracellular space and defend against bacteria passage.[2] IECs are covered with a 2-layer mucus barrier, which forms the first line of defense in the intestinal mucosal barrier. The loose outer mucus layer provides a natural habitat for commensal bacteria. The dense inner mucus layer is firmly attached to epithelial cells and does not allow commensal microbes to penetrate, forming the primary structure of the mucus barrier.[3]

Inflammatory bowel diseases (IBDs), including Crohn's disease and ulcerative colitis, are characterized by dysfunction of the mucosal barrier and alterations in microbial community.[4] The inner mucus layer is attenuated and can be penetrated by commensal bacteria in IBD patients and dextran sodium sulfate (DSS)-induced colitis mouse models. The variable bacteria that attached to and penetrated IECs can activate immune responses to produce inflammatory cytokines, including interferon-γ and tumor necrosis factor α (TNF-α), which can increase epithelial permeability and induce epithelial barrier dysfunction by disrupting epithelial cell junctions.[5] The immune responses activated by defective mucosal barriers and microbial dysbiosis promote the accumulation of inflammatory signals, causing chronic or recurrent relapsing colonic inflammation, pathologic proliferation and apoptosis in epithelium, and even triggering tumorigenesis of colon cancer.[6–9]

As the major component of the mucus layer, Mucin-2 (MUC2) is generated by goblet cells. An appropriate number of goblet cells and their proper functions in MUC2 synthesis, folding, and secretion are essential for maintaining the mucus layer. Indeed, dysfunctions in goblet cells are the known characteristics of IBD.[10–13] The glycosylation and folding of MUC2 in endoplasmic reticulum (ER) are controlled by calreticulin and calnexin, which require steady ER–Ca^{2+} homeostasis.[14–17] Disturbed ER–Ca^{2+} homeostasis can affect the calnexin/calreticulin pathway,[18] causing MUC2 misfolding in ER. Furthermore, aberrant MUC2 folding induces ER stress in goblet cells.[19] Studies in murine models have shown that severe or chronic ER stress can lead to goblet cell apoptosis, which further impairs the mucus layer and increases microbial exposure, confirming that abnormal ER stress is one of the triggers for the pathogenesis of IBD.[20–22] Hence, ameliorating goblet cell ER stress by maintaining ER–Ca^{2+} homeostasis is regarded as a potential interventional strategy to alleviate colitis.

Stromal interaction molecule 1 (STIM1) is the major component of store-operated Ca^{2+} entry (SOCE) to mediate Ca^{2+} influx by sensing Ca^{2+} reductions in ER and gating ORAI calcium release-activated calcium modulator (ORAI) channels in plasma membrane. Previous studies have shown that STIM1 is overexpressed in many cancers, including colorectal cancer.[23] STIM1 boosts the production of proinflammatory cytokines, especially cyclooxygenase 2, to enhance the progression and motility of colorectal cancer, indicating that STIM1 promotes the inflammatory response during tumorigenesis.[23] In lung endothelial cells, blockade of STIM1 significantly reduced lipopolysaccharide-induced lung inflammation. Ca^{2+} oscillations and nuclear factor of activated T Cells (NFAT) - nuclear accumulation were abrogated in STIM1$^{\Delta EC}$ mice, thereby leading to the decrease in proinflammatory signaling and oxidative stress.[24] Moreover, STIM1 is essential for the differentiation and function of T cells. STIM1-deficient T cells were incapable of inducing autoimmunity in autoimmune diseases, including IBD, owing to impaired helper T cell 17 effector functions. Other studies further confirmed that STIM1 could facilitate pathogenic helper T cell 17 cells to exacerbate intestinal inflammation.[25–28] Consistently, the STIM1-mediated SOCE in T cells isolated from the lamina propria (LP) of IBD patients was increased when compared with that of healthy individuals.[29]

In this study, we collected intestinal tissues from IBD patients and confirmed the overexpression of STIM1 in inflammatory tissues. To investigate the effects of intestinal

*Authors share co-first authorship.

Abbreviations used in this paper: **CAC, colitis-associated colorectal cancer; Cdh1, Cadherin 1; DSS, dextran sodium sulfate; ER, endoplasmic reticulum; FBS, fetal bovine serum; FITC, fluorescein isothiocyanate; HBSS, Hank's balanced salt solution; IBD, inflammatory bowel disease; IEC, intestinal epithelial cell; IHC, immunohistochemistry; IL, interleukin; LP, lamina propria; mLN, mesenteric lymph node; mRNA, messenger RNA; MUC2, Mucin-2; ORAI, ORAI calcium release-activated calcium modulator; PAS, periodic acid–Schiff; PBS, phosphate-buffered saline; qPCR, quantitative polymerase chain reaction; sIgA, secretory IgA; SOCE, store-operated Ca^{2+} entry; STIM1, stromal interaction molecule 1; STIM1$^{f/f}$, wild type littermates of STIM1$^{\Delta IEC}$_mice; STIM1$^{\Delta IEC}$, intestinal epithelium-specific STIM1 conditional knockout mice; TG, thapsigargin; Tm, tunicamycin; TNF-α, tumor necrosis factor α; UEA-1, ulex europaeus agglutinin-1; WB, Western Blots; ZO1, Zonula Occludens 1.**

Most current article

2352-345X
https://doi.org/10.1016/j.jcmgh.2022.03.007

mucosal STIM1 in IBD, we generated intestinal epithelium-specific STIM1 conditional knockout mice ($STIM1^{\Delta IEC}$) and identified the important role of intestinal epithelial STIM1 in promoting colitis. STIM1 deficiency specifically in intestinal epithelium significantly reduced goblet cell loss through the inhibition of ER stress, maintaining the integrity of the inner mucus layer, protecting intestinal epithelium from the stimulation by commensal bacteria, and thereby alleviating DSS-induced colitis and tumorigenesis of colitis-associated colorectal cancer (CAC).

Results

Enhanced Expression of STIM1 in IBD Patients

STIM1 has been confirmed to be overexpressed in various cancers, but the expression level of STIM1 protein in IBD patients has not been reported. We collected inflammatory and matched-adjacent normal intestinal tissues from IBD patients. Western Blots (WB) results showed that STIM1 was expressed at significantly higher level in inflammatory tissues than that in matched normal tissues (Figure 1*A*), immunohistochemistry (IHC) and immunofluorescence results showed that the overexpression of STIM1 was found in both IECs and LP (Figure 1*B*–*F*).

STIM1 Deficiency in Intestinal Epithelium Has No Effect on Mouse Growth or Epithelial Differentiation

Previous results have confirmed that STIM1-mediated SOCE in LP of IBD patients was increased,[29] but enhanced STIM1 in IECs of IBD patients was found. To identify the role of epithelia STIM1 in intestinal inflammation, we generated $STIM1^{\Delta IEC}$ mice with conditional deletion of STIM1 in intestinal epithelia. Quantitative polymerase chain reaction (qPCR), WB and IHC assays were performed to verify STIM1 knockout. We found that STIM1 expression level was substantially and specifically reduced in intestinal epithelium of $STIM1^{\Delta IEC}$ mice (Figure 2*A*–*D*). Next, we detected the body weight, colonic villus height, ORAI1 expression, and genes related to epithelial differentiation between $STIM1^{\Delta IEC}$ mice and their wild-type littermates, and observed no significant difference (Figure 2*E*–*K*). These results indicate that STIM1 ablation in intestinal epithelium has no effect on mouse growth or epithelial differentiation.

STIM1 Deficiency in Intestinal Epithelium Alleviates DSS-Induced Colitis

To identify the role of STIM1 in colitis development, $STIM1^{\Delta IEC}$ mice and their wild type littermates ($STIM1^{f/f}$) were administered 2% DSS to induce colitis. STIM1 depletion in intestinal epithelium led to a protective effect during DSS treatment. The weight loss of $STIM1^{\Delta IEC}$ mice was lower than that of $STIM1^{f/f}$ mice after DSS removal. On day 9, the body weights of most $STIM1^{\Delta IEC}$ mice began to recover, whereas all $STIM1^{f/f}$ mice still suffered sustained weight loss (Figure 3*A*). In addition, the disease activity index, which reflected weight loss, stool consistency, and fecal blood presence, also was decreased in $STIM1^{\Delta IEC}$ mice (Figure 3*B*). Other clinical parameters that indicate colitis severity, such as splenomegaly and colon length, were assessed, and the results further indicated that STIM1 deficiency in intestinal epithelium reduced the susceptibility to DSS-induced colitis (Figure 3*C*–*E*). Histologically, the colon tissues of $STIM1^{\Delta IEC}$ mice maintained basic structure, with mild inflammatory cell infiltration and ulceration. By contrast, $STIM1^{f/f}$ mice showed severe ulceration, massive inflammatory cell infiltration, and complete loss of epithelial structure, resulting in a higher histologic activity index (Figure 3*F* and *G*).

To confirm the role of STIM1, we examined the inflammatory cytokines of experimental mice. A previous study reported increased serum secretory IgA (sIgA) in IBD patients[30]; in this study, we detected a 4-fold reduction of serum sIgA level in $STIM1^{\Delta IEC}$ mice (Figure 3*H*). Interleukin (IL)6 and TNF-α were decreased in the sera, colon tissues, spleen, mesenteric lymph node (mLN), and thymus of $STIM1^{\Delta IEC}$ mice, although the difference in TNF-α levels was not statistically significant (Figure 4*A*–*E*). In addition, qPCR analyses of inflammatory cytokines in colon tissues showed that $STIM1^{\Delta IEC}$ mice produced lower levels of IL1β, IL6, TNF-α, inducible nitric oxide synthase, cyclooxygenase 2, and cathelicidin antimicrobial peptide (Camp) than $STIM1^{f/f}$ mice (Figure 4*F*).

Collectively, these results suggest that STIM1 deficiency in intestinal epithelium alleviates DSS-induced colitis.

STIM1 Deficiency in Intestinal Epithelium Facilitates Epithelial Barrier Maintenance

To explore the mechanism by which colitis is alleviated in $STIM1^{\Delta IEC}$ mice, we analyzed differential gene expression of colon tissues from DSS-treated mice by RNA sequencing. The results showed great distinction between $STIM1^{f/f}$ and $STIM1^{\Delta IEC}$ mice (Figure 5*A*). Gene Ontology analysis of differentially expressed genes between $STIM1^{f/f}$ and $STIM1^{\Delta IEC}$ mice identified significant enrichment in cell adhesion and cell junction among biological processes and cellular components (Figure 5*B* and *C*). Kyoto Encyclopedia of Genes and Genomes pathway analysis showed enriched cell adhesion molecules and extracellular matrix–receptor interaction (Figure 5*D*). Furthermore, genes related to cell junctions, which are essential for epithelial barrier,[2] including *Cadherin 1* (*Cdh1*), *Zonula Occludens 3* (*ZO3*), *occludin*, *Cldn2*, *Cldn3*, *Cldn7*, *Cldn8*, and *Cldn15*, were upregulated in $STIM1^{\Delta IEC}$ mice (Figure 5*E*). These results indicated that STIM1 deficiency in the intestinal epithelium is beneficial for the maintenance of integrated epithelial barrier.

To further confirm the role of STIM1 in the epithelial barrier, fluorescein isothiocyanate (FITC)–dextran was used to examine intestinal permeability. The decreased FITC–dextran level in the serum of $STIM1^{\Delta IEC}$ mice showed a more integrated epithelial barrier in $STIM1^{\Delta IEC}$ mice than that in $STIM1^{f/f}$ mice with DSS administration (Figure 6*A*).

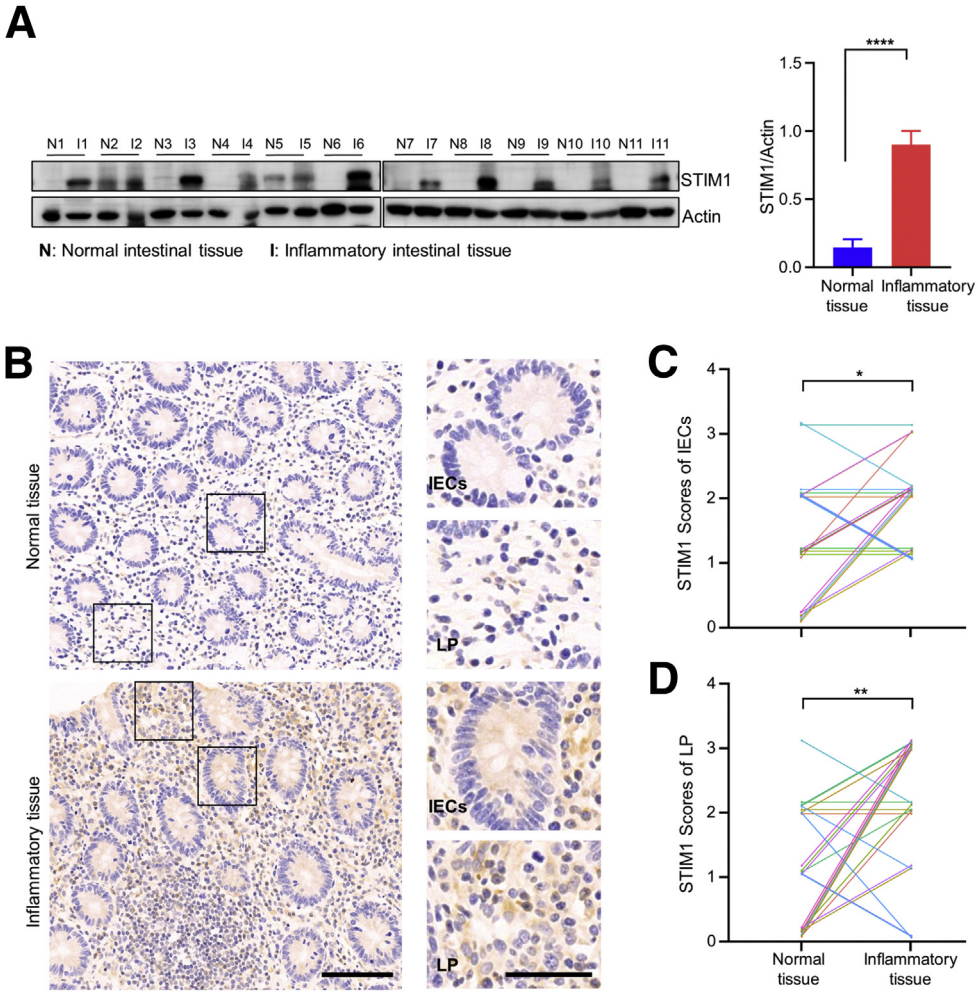

Figure 1. Enhanced expression of STIM1 in IBD patients. (*A*) Protein expression of STIM1 in inflammatory and matched-adjacent normal intestinal tissues from IBD patients. (*B–D*) IHC staining and IHC scores showing STIM1 expression in IECs and LP of IBD patients (n = 25). *Scale bars*: 100 μm, *boxed pullout*: 50 μm. Twenty-five random numbers between 0 and 0.2 were generated and added to the IHC score of each sample to avoid an overlap of points. (*E*) Representative immunofluorescence of CD45 (green) and STIM1 (red) in intestinal tissues from IBD patients. *Scale bars*: 100 μm. (*F*) Representative immunofluorescence of EpCAM (green) and STIM1 (red) in intestinal tissues from IBD patients. *Scale bars*: 100 μm. The results are presented as the means ± SEM. ****$P <$ .0001, **$P < 0.01$, and *$P <$ .05. (*C* and *D*) Paired Student *t* test for IHC scores without random numbers. DAPI, 4′,6-diamidino-2-phenylindole.

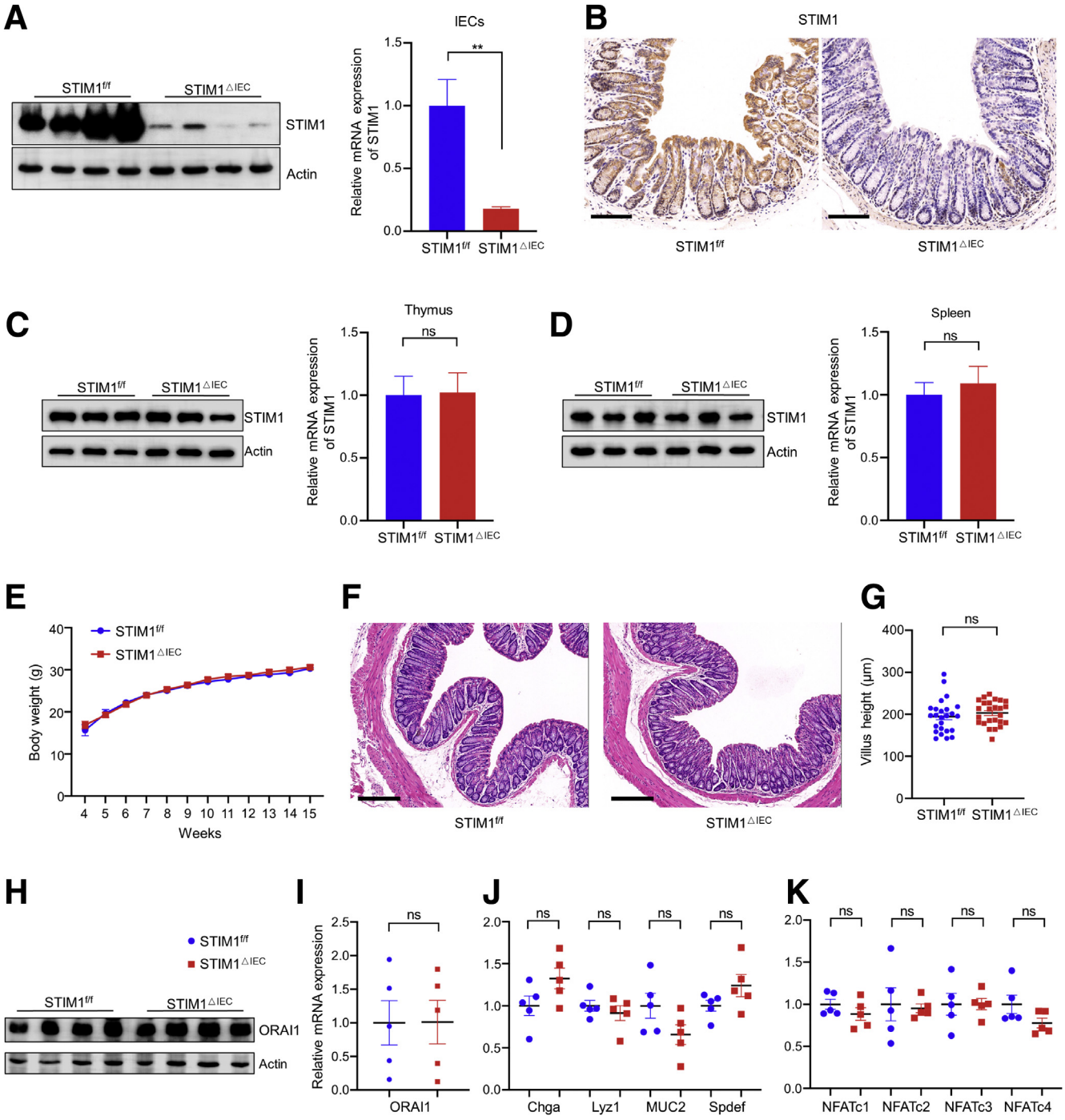

Figure 2. STIM1 deficiency in intestinal epithelium has no effect on mouse growth or epithelial differentiation. WB and qPCR analysis of (*A*) IECs, (*C*) thymus, and (*D*) spleen lysates from STIM1$^{f/f}$ and STIM1$^{\Delta IEC}$ mice. (*B*) Immunostaining for STIM1 in the colons of STIM1$^{f/f}$ and STIM1$^{\Delta IEC}$ mice (n = 4 per group). *Scale bars*: 100 μm. (*E*) Body weight changes in STIM1$^{f/f}$ and STIM1$^{\Delta IEC}$ male mice over time (n = 6 per group). Representative (*F*) H&E staining and (*G*) villus height in the distal colons of STIM1$^{f/f}$ and STIM1$^{\Delta IEC}$ mice at 10 weeks of age (n = 5 per group; 5 regions of interest per mouse). *Scale bars*: 200 μm. (*H*) WB and (*I*) qPCR analysis of ORAI1 in IECs of STIM1$^{f/f}$ and STIM1$^{\Delta IEC}$ mice (n = 4–5 per group). (*J* and *K*) Relative mRNA expression of the indicated genes in the IECs of STIM1$^{f/f}$ and STIM1$^{\Delta IEC}$ mice (n = 5 per group). The results are shown as the means ± SEM. $^{**}P < .01$, NS at $P > .05$.

Consistently, with DSS treatment, messenger RNA (mRNA) levels of cell adhesion genes, including *occludin*, *Cdh1*, *zonula occludens*, and *claudins*, were up-regulated in STIM1$^{\Delta IEC}$ mice IECs, which corresponded with the significantly up-regulated protein levels of occludin, Cdh1, and Zonula Occludens 1 (ZO1) in STIM1$^{\Delta IEC}$ mice IECs

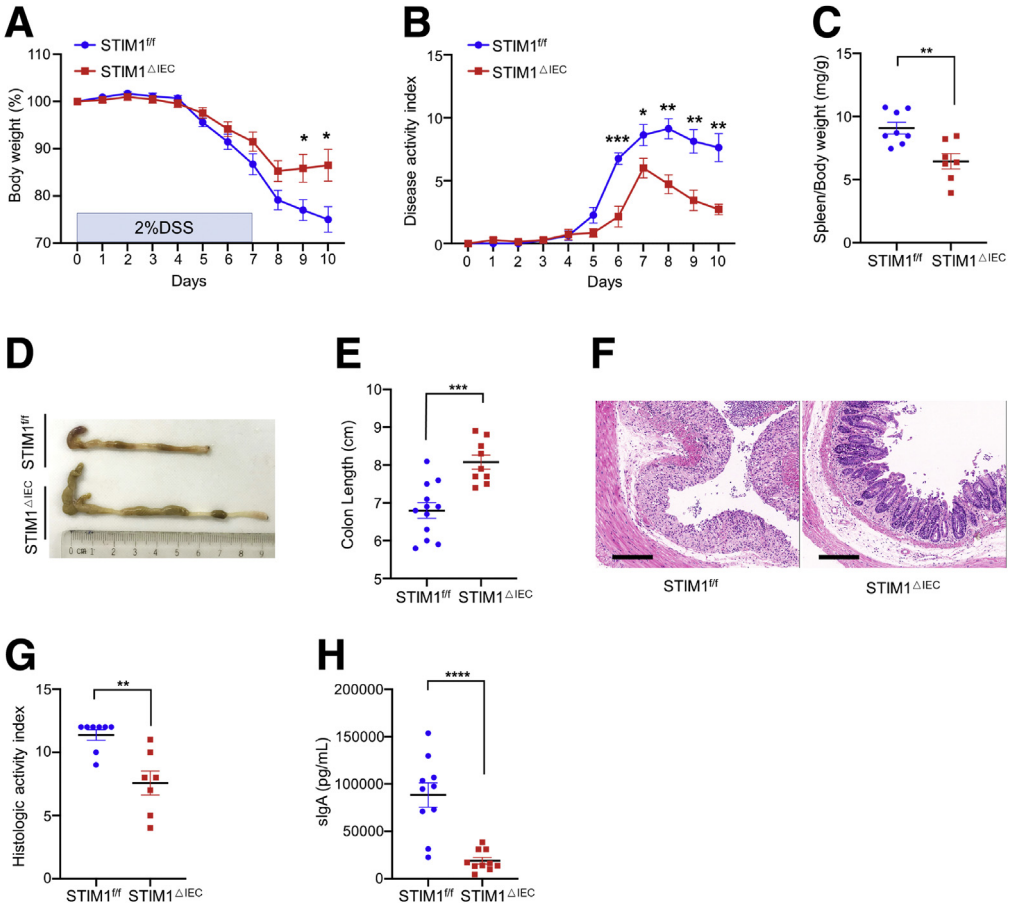

Figure 3. STIM1 deficiency in intestinal epithelium alleviates DSS-induced colitis. The percentage change in (*A*) body weight and (*B*) disease activity index during DSS-induced colitis (n = 7–8 per group). (*C*) Splenomegaly was indicated by spleen/body weight on day 10 (n = 7–8 per group). (*D* and *E*) Colon length on day 10 (n = 9–12 per group). (*F* and *G*) Representative H&E staining of colon sections and the histologic activity index on day 10 (n = 7–8 per group). *Scale bar*: 200 μm. (*H*) Serum levels of sIgA on day 10 (n = 10 per group). Results are presented as the means ± SEM. *****P* < .0001, ****P* < .001, ***P* < .01, and **P* < .05.

(Figure 6*B*–*E*). IHC was used to further confirm the expression levels of Cdh1 and occludin in intestinal epithelial tissues. The results showed that STIM1 deficiency in intestinal epithelium did not affect the epithelial barrier in the steady state. However, on day 10 after exposure to DSS, there was a significant difference in the expression of Cdh1 and occludin between $STIM1^{f/f}$ and $STIM1^{\Delta IEC}$ mice (Cdh1, 1.06% vs 18.95%; occludin, 1.83% vs 14.14%) (Figure 6*F*–*I*). These data show that STIM1 deficiency in the intestinal epithelium effectively protects the epithelial barrier against DSS-induced dysfunction.

STIM1 Deficiency in Intestinal Epithelium Protects Colonic Inner Mucus Against DSS-Induced Damage

Colonic IECs are covered by 2 layers of mucus, the outer mucus layer is loose and forms a habitat for commensal bacteria, while the inner mucus layer is dense and tightly attached to epithelial cells, forming the first line of defense to prevent contact between epithelium and luminal flora.[3]

Because adherens and tight junction molecules of the epithelial barrier were altered in DSS-treated $STIM1^{\Delta IEC}$ mice (Figures 5 and 6), we examined the inner mucus layer in DSS-treated mice to investigate whether the first line of defense was affected. Strikingly, results of Alcian blue/periodic acid–Schiff (PAS) staining showed that $STIM1^{\Delta IEC}$ mice had thicker mucus than $STIM1^{f/f}$ mice on day 7 (Figure 7*A* and *B*). To further verify the alterations in the inner mucus layer, we visualized the mucosal surface using scanning electron microscopy and found that the mucosal surface of $STIM1^{\Delta IEC}$ mice was covered with rich mucus, in contrast to the bare surface and exposed microvilli of $STIM1^{f/f}$ mice (Figure 7*C*). Immunostaining of ulex europaeus agglutinin-1 (UEA-1), which is specific for fucose lectin in mucus secreted by goblet cells and can be used to indicate the mucus layer, also showed a dense and integrated mucus layer in $STIM1^{\Delta IEC}$ mice, while mucus in $STIM1^{f/f}$ mice was interrupted and weakly stained (Figure 7*D* and *E*), indicating that STIM1 deficiency in intestinal epithelium protects colonic mucus against DSS-induced damage.

STIM1 Deficiency in Intestinal Epithelium Sustains the Integrity of Inner Mucus Layer by Alleviating Goblet Cell Loss

Mucins are generated by goblet cells, for which we hypothesized that STIM1 may affect the function of goblet cells.

First, we examined the mRNA levels of SAM pointed domain containing ETS transcription factor (*Spdef*), atonal

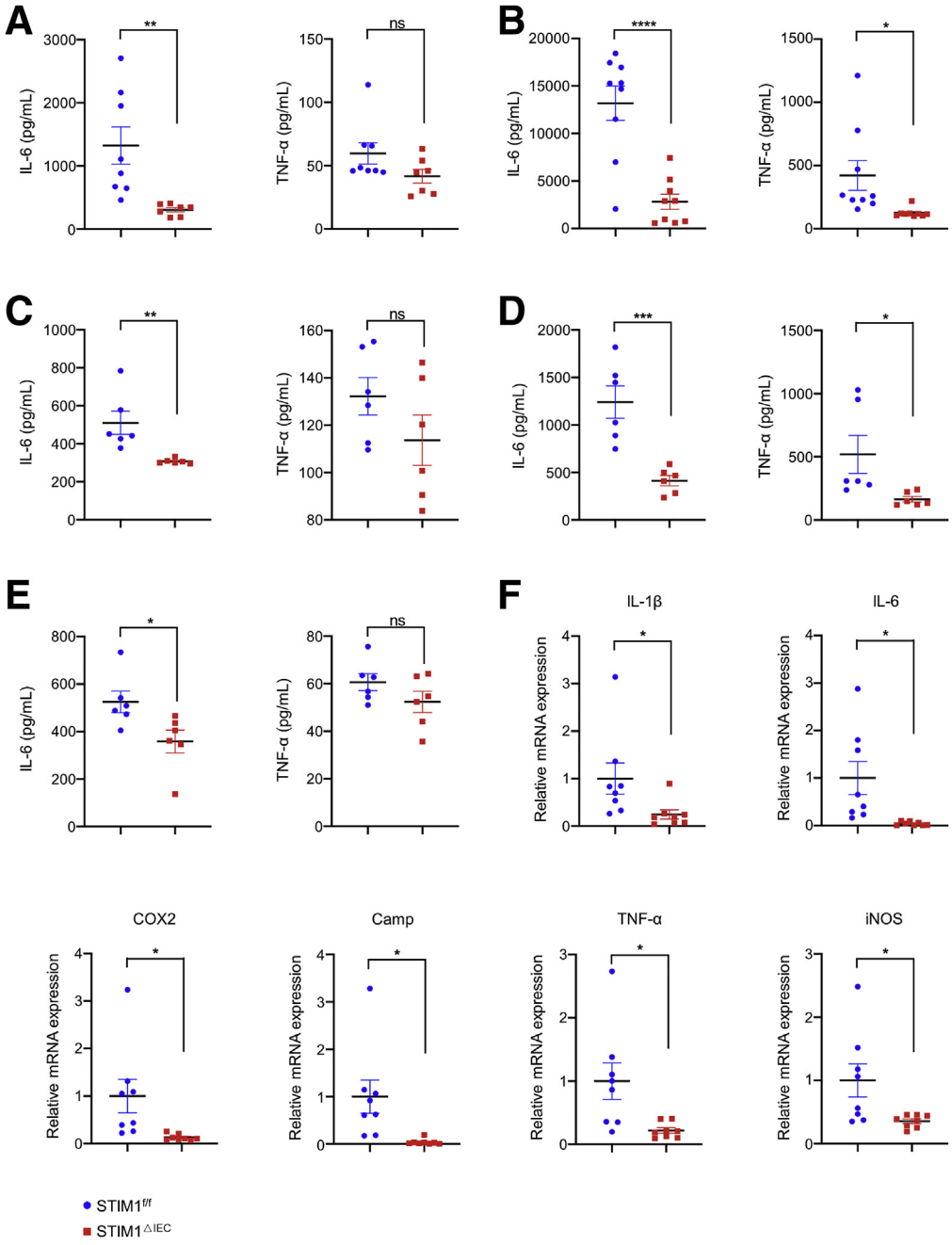

Figure 4. STIM1 deficiency in intestinal epithelium alleviates the production of inflammatory cytokines. (*A*) Serum levels of IL6 and TNF-α on day 10 of DSS administration (n = 7–8 per group). (*B*) IL6 and TNF-α levels in colon tissue supernatants on day 10 (n = 9 per group). (*C*) IL6 and TNF-α levels in spleen supernatants on day 10 (n = 6 per group). (*D*) IL6 and TNF-α levels in mLN supernatants on day 10 (n = 6 per group). (*E*) IL6 and TNF-α levels in thymus supernatants on day 10 (n = 6 per group). (*F*) Relative mRNA expression of inflammatory cytokines in colon tissues on day 10 (n = 8 per group). Data are presented as the means ± SEM. ****$P < .0001$, ***$P < .001$, **$P < .01$, and *$P < .05$; NS at $P > .05$. COX2, cyclooxygenase 2; iNOS, inducible nitric oxide synthase; Camp, cathelicidin antimicrobial peptide.

BHLH transcription factor 1 (*Atoh1*), kruppel like factor 4 (*Klf4*), and hes family BHLH transcription factor 1 (*Hes1*), the key factors for differentiation and maturation of goblet cells,[13] and found no difference between DSS-treated STIM1$^{\Delta IEC}$ and STIM1$^{f/f}$ mice (Figure 8*A*). IL10 can promote the production of inner mucus by suppressing the misfolding of mucins in goblet cells[31]; however, although a wide range of cytokines were decreased in DSS-treated STIM1$^{\Delta IEC}$ mice (Figure 4), the expression level of IL10 was not altered significantly (Figure 8*B*), refuting the surmise that STIM1 deficiency in intestinal epithelium promotes the correct mucin folding by affecting the expression of IL10. Next, we explored whether STIM1 had effects on goblet cell secretion. However, transmission electron microscopy images showed that the release of mucin granules in apical goblet cells of STIM1$^{\Delta IEC}$ mice was similar to that of STIM1$^{f/f}$ mice (Figure 8*C*).

These results showed that STIM1 deficiency in the intestinal epithelium had no effect on goblet cell differentiation, maturation, or secretion in the development of colitis. However, the number of PAS-positive cells per crypt was significantly higher in STIM1$^{\Delta IEC}$ mice than in STIM1$^{f/f}$ mice (5.9 vs 1.5 per crypt, respectively) (Figure 8*D* and *E*), indicating that STIM1 affects the number of goblet cells during colitis. Consistently, PAS assay also showed more PAS-positive products in the colon tissues of STIM1$^{\Delta IEC}$ mice

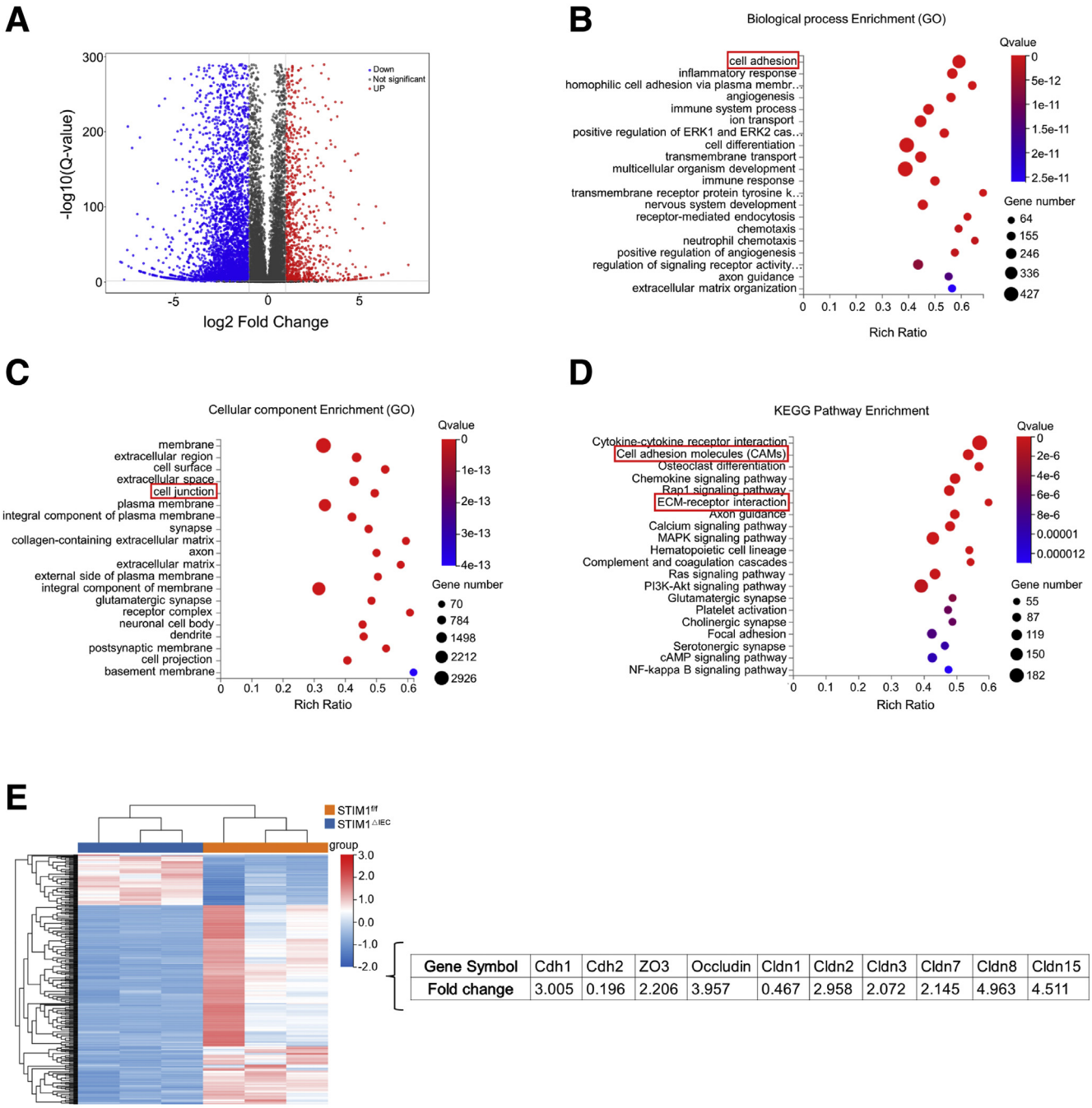

Gene Symbol	Cdh1	Cdh2	ZO3	Occludin	Cldn1	Cldn2	Cldn3	Cldn7	Cldn8	Cldn15
Fold change	3.005	0.196	2.206	3.957	0.467	2.958	2.072	2.145	4.963	4.511

Figure 5. Alterations in epithelial barrier in STIM1-deficient mice during DSS-induced colitis. RNA sequencing of DSS-treated mice was performed (n = 3 per group). (*A*) Volcano plot showing genes with different expression levels in colon tissues of STIM1$^{\Delta IEC}$ mice compared with STIM1$^{f/f}$ mice. Differentially expressed genes (DEGs) with false discovery rate (FDR) = 0 makes values of logarithm infinite are not shown. (*B–D*) Biological process enrichment (Gene Ontology [GO]), cellular component enrichment (GO), and Kyoto Encyclopedia of Genes and Genomes (KEGG) pathway enrichment analysis of differently expressed genes with a greater than 2-fold change. (*E*) Heat map showing genes related to cell junctions. cAMP, cyclic adenosine monophosphate; ECM, extracellular matrix; ERK, extracellular signal-regulated kinase; MAPK, mitogen-activated protein kinases; NF, nuclear factor.

(Figure 8*F*). MUC2 and anterior gradient 2 (AGR2), considered the components of mucus and generated by goblet cells,[32] showed similar trends in gene expression with the change in goblet cell number (Figure 8*G* and *H*).

Collectively, these results indicate that STIM1 deficiency in the intestinal epithelium maintains the inner mucus layer integrity in DSS-induced colitis by alleviating goblet cell loss.

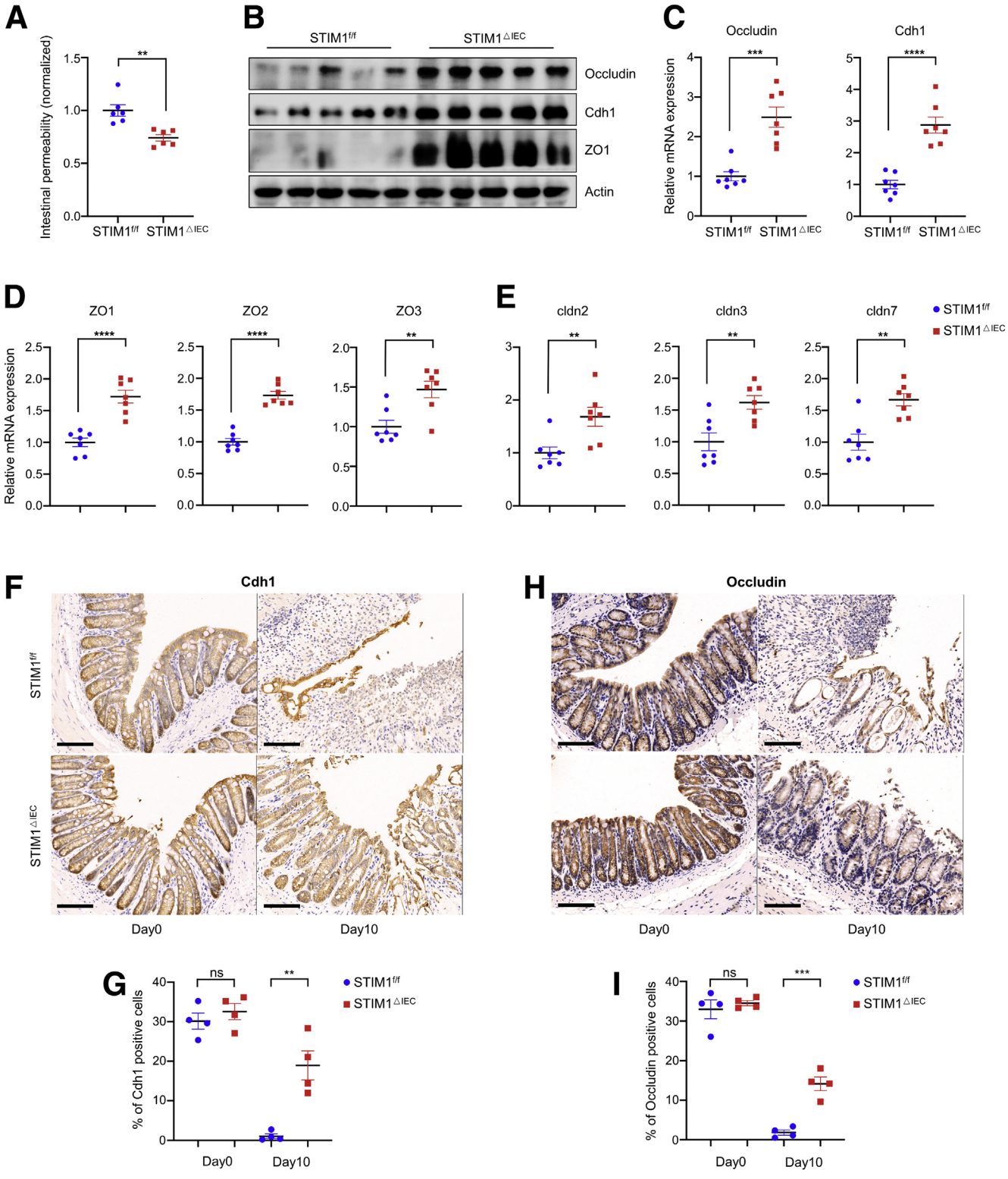

Figure 6. STIM1 deficiency in intestinal epithelium facilitates epithelial barrier maintenance. (*A*) Intestinal permeability was assessed by FITC–dextran assays on day 7 of DSS administration (n = 6 per group). (*B*) The expression of tight junctions was assessed using WB (n = 5 per group) for occludin, Cdh1, and ZO1 in IECs on day 7. (*C–E*) Relative mRNA expression of occludin, Cdh1, zonula occludens, and claudins in the IECs of $STIM1^{f/f}$ and $STIM1^{\Delta IEC}$ mice on day 7 (n = 7 per group). (*F–I*) IHC staining and quantification of Cdh1- and occludin-positive cells on day 0 and day 10 (n = 4 per group). *Scale bars*: 100 μm. Data are presented as the means ± SEM. $^{****}P < .0001$, $^{***}P < .001$, and $^{**}P < .01$; NS at $> .05$.

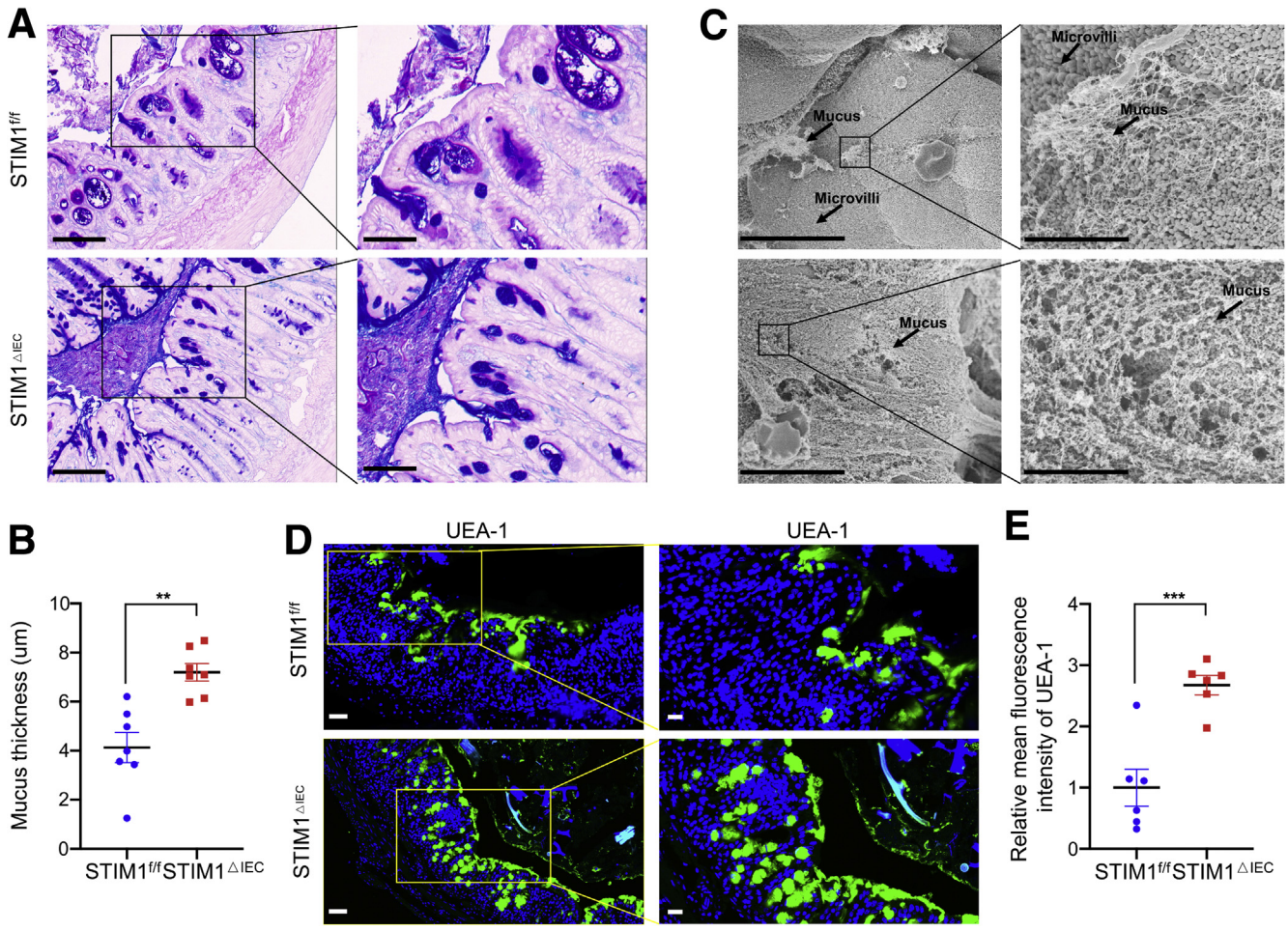

Figure 7. STIM1 deficiency in intestinal epithelium protects colonic inner mucus against DSS-induced damage. (*A*) Representative images of Alcian blue/PAS-stained distal colon sections from STIM1$^{f/f}$ and STIM1$^{\Delta IEC}$ mice on day 7 of DSS administration, showing the inner mucus (n = 7 per group). *Scale bars*: 100 μm, *boxed pullout*: 50 μm. (*B*) Measurement of inner mucus thickness in distal colon (n = 7 per group). (*C*) Scanning electron microscopy of unwashed colonic epithelial surface from DSS-treated mice on day 7. *Scale bars*: 10 μm, *boxed pullout*: 2 μm. (*D* and *E*) Immunofluorescence staining and mean fluorescence intensity for UEA-1 of distal colon section on day 7 to visualize the inner mucus and mucins (n = 6 per group). *Scale bars*: 50 μm, *boxed pullout*: 20 μm. Data are presented as the means ± SEM. ***$P < .001$ and **$P < .01$.

STIM1 Deficiency in Colonic Goblets Cells Alleviates ER Stress and Subsequent Cell Apoptosis by Reducing Ca^{2+} Overload

Mucins, especially MUC2, are large and complex glycoproteins that can increase the probability of protein misfolding during ER biosynthesis in goblet cells. Murine models show that MUC2 misfolding within ER causes ER stress in goblet cells, and prolonged ER stress leads to goblet cell loss and spontaneous colitis. The high expression of MUC2 makes goblet cells the initial IECs that undergo ER stress and subsequent apoptosis during DSS treatment, eventually leading to depleted and defective mucus and driving colitis susceptibility.[11,19–22,33]

Because STIM1$^{\Delta IEC}$ mice showed reduced goblet cell loss during DSS-induced colitis, we hypothesized that this effect was the consequence of ER stress inhibition in goblet cells. Consistent with our speculation, during DSS treatment, the mRNA levels of genes related to ER stress induced by protein misfolding, especially *IRE1* and *CHOP*, the fundamental ER stress signals that initiate and promote apoptosis,[34] were significantly lower in the colons of STIM1$^{\Delta IEC}$ mice (Figure 9*A*). WB analysis also showed decreased IRE1α and CHOP protein expression in STIM1$^{\Delta IEC}$ mice (Figure 9*B*). In addition, UEA-1 and CHOP protein levels were detected on day 7 of DSS administration, as shown by immunofluorescence staining, and the decreased expression of CHOP in goblet cells (UEA-1–positive cells) of STIM1$^{\Delta IEC}$ mice showed reduced ER stress in goblet cells (Figure 9*C*). The decreased expression of cleaved-Caspase 3 (C-Caspase 3) in goblet cells further suggested the inhibited apoptosis of goblet cells in STIM1$^{\Delta IEC}$ mice (Figure 9*D*).

To further confirm the role of STIM1 in ER stress and prolonged ER stress–induced apoptosis of goblet cells, we used human colonic LS174T cells that produce large amounts of MUC2 as an in vitro model of intestinal goblet

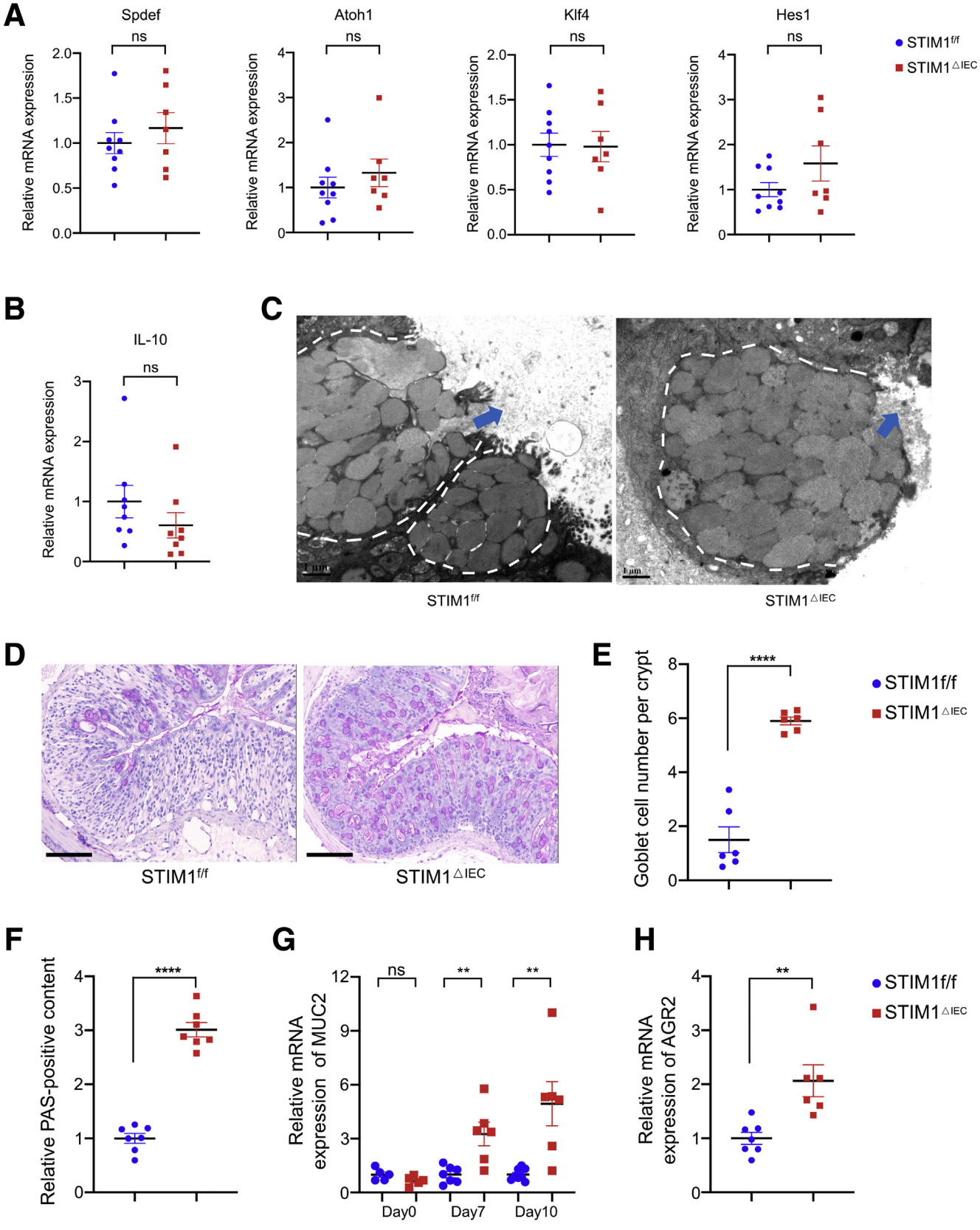
A
Spdef
Atoh1
Klf4
Hes1
ns
Relative mRNA expression
STIM1f/f
STIM1△IEC
B
IL-10
C
STIM1f/f
STIM1△IEC
D
E
Goblet cell number per crypt
****
F
Relative PAS-positive content
G
Relative mRNA expression of MUC2
**
Day0
Day7
Day10
H
Relative mRNA expression of AGR2

cells.[31] The ER stress of cells with or without STIM1 deficiency was induced by tunicamycin (Tm) or thapsigargin (TG). The results showed that STIM1 knockdown significantly decreased the up-regulation of ER stress markers induced by Tm or TG at both protein and mRNA levels, including *CHOP*, *IRE1α*, *Bip*, *PERK*, and *ATF4* (Figure 10*A* and *B*). Furthermore, STIM1 deficiency effectively reduced the apoptosis of LS174T cells induced by ER stressors (Figure 10*C* and *D*). ER stress is elicited by disturbance of ER–Ca^{2+} homeostasis accompanied by intracellular Ca^{2+} overload, which further exacerbates ER stress and results in apoptosis.[35] Hence, we examined changes in intracellular Ca^{2+} influx induced by Tm or TG in LS174T cells and determined that STIM1 knockdown significantly reduced ER stressor–induced Ca^{2+} overload (Figure 10*E* and *F*), suggesting that STIM1 deficiency alleviates ER stress by reducing Ca^{2+} overload.

Both in vivo and in vitro models showed that STIM1 deficiency in goblet cells decreased their susceptibility to ER stress and inhibited subsequent cell apoptosis, suggesting that STIM1 deficiency in intestinal epithelium alleviates goblet cell loss by inhibiting ER stress.

STIM1 Deficiency in Intestinal Epithelium Protects Intestinal Epithelium Against Stimulation of Commensal Bacteria

Under physiological conditions, the inner mucus layer prevents contact between the intestinal epithelium and commensal bacteria and the outer mucus layer acts as a habitat and food source for commensal bacteria.[3] During DSS treatment, bacteria could penetrate the inner mucus layer immediately before inflammatory reactions and attach to the intestinal epithelium to aggravate colonic inflammation and even trigger the development of colon cancer.[6,7,9,36–38] Moreover, microbial community is altered in colitis, which can affect mucus glycosylation and promote the development of intestinal inflammation.[1,39]

Therefore, we examined the intestinal microbial community to investigate whether the commensal bacteria is the inducer of colitis distinction in $STIM1^{\Delta IEC}$ and $STIM1^{f/f}$ mice. A 16S sequence analysis of stool samples showed similar β-diversity between DSS-treated $STIM1^{\Delta IEC}$ and $STIM1^{f/f}$ mice using principal component analysis (Figure 11*A*). However, at the phylum level, *Bacteroidetes* were slightly more abundant and *Proteobacteria* were slightly less abundant in $STIM1^{\Delta IEC}$ mice compared with $STIM1^{f/f}$ mice (Figure 11*B*), consistent with the fecal bacterial changes reported in healthy controls compared with IBD patients.[40,41] At the genus level, $STIM1^{\Delta IEC}$ mice showed a decreasing trend in potential pathogenic bacteria, including *Escherichia–Shigella* and *Helicobacter*, and an increasing trend in beneficial bacterial species, including *Lactobacillus* and *Ruminococcaceae* (Figure 11*C* and *D*).

Although these data suggested that STIM1 deficiency in intestinal epithelium provided a stable environment for promoting beneficial bacteria and hindering potential pathogenic species during DSS treatment, the slight alteration with no statistical difference in commensal bacteria indicated that the change of their species was not a potent inducer of the colitis distinction between $STIM1^{\Delta IEC}$ and $STIM1^{f/f}$ mice. Next, we applied an EUB338 DNA probe to detect the distances between bacteria and intestinal epithelium in DSS-treated mice and observed that commensal bacteria were prevented from penetrating the mucus layer or attaching to the epithelium of $STIM1^{\Delta IEC}$ mice (Figure 12*A*), thereby leading to significant inhibition of pathogenic bacterial translocation from the bowel lumen to colon tissue, liver, spleen, and mLN (Figure 12*B*), and the inhibition was benefit from integrated inner mucus layer (Figure 7).

These results indicated that STIM1 deficiency in the intestinal epithelium protects the intestinal epithelium against stimulation of commensal bacteria through regulating the inner mucus layer rather than changing the bacterial community, and thereby alleviates colonic inflammation exacerbated by bacterial stimulation.

STIM1 Deficiency in Intestinal Epithelium Promotes the Recovery From Colitis and Renders Mice Less Susceptible to Colitis-Associated Colorectal Cancer

The integrated inner mucus layer can protect intestinal epithelium against chronic inflammation stimulated by commensal bacteria and thereby prevent subsequent colorectal tumorigenesis.[9] Hence, we explored whether STIM1 deficiency in intestinal epithelium decreased the occurrence of CAC developed from chronic inflammation.

We examined the colitis convalescence of $STIM1^{\Delta IEC}$ and $STIM1^{f/f}$ mice to investigate whether the process of chronic inflammation was altered. In $STIM1^{f/f}$ mice, the epithelium was stimulated continuously by commensal bacteria during colitis because of the defective inner mucus layer (Figures 7 and 12), leading to further exacerbated colitis and slow

Figure 8. (***See previous page***). **STIM1 deficiency in intestinal epithelium sustains the inner mucus layer integrity by alleviating goblet cell loss.** (*A*) Relative mRNA levels of the indicated transcription factors associated with differentiation and maturation of goblet cells in IECs on day 7 of DSS administration (n = 7–9 per group). (*B*) Relative mRNA expression of IL10 in colon tissues on day 10 (n = 8 per group). (*C*) Representative transmission electron microscopy images of apical goblet cells on day 7. The *dashed white line* highlights the goblet cell edge, the *blue arrow* indicates the vesicular secretion. *Scale bars*: 1 μm. (*D* and *E*) PAS staining of distal colon sections on day 7 and the quantification of PAS-positive goblet cells per crypt (n = 6 per group). *Scale bars*: 100 μm. (*F*) PAS assay results indicating the relative expression of PAS-positive content on day 7 (n = 7 per group). (*G*) Relative mRNA expression of MUC2 in the IECs of $STIM1^{f/f}$ and $STIM1^{\Delta IEC}$ mice on day 0, day 7, and day 10. The data were normalized to $STIM1^{f/f}$ mice (day 0, n = 5 per group; day 7, n = 6–7 per group; and day 10, n = 6–8 per group). (*H*) Relative mRNA expression of AGR2 in IECs on day 7 (n = 6–7 per group). Results are presented as the means ± SEM. $^{****}P < .0001$, $^{**}P < .01$; NS at $P > .05$. AGR2, anterior gradient 2.

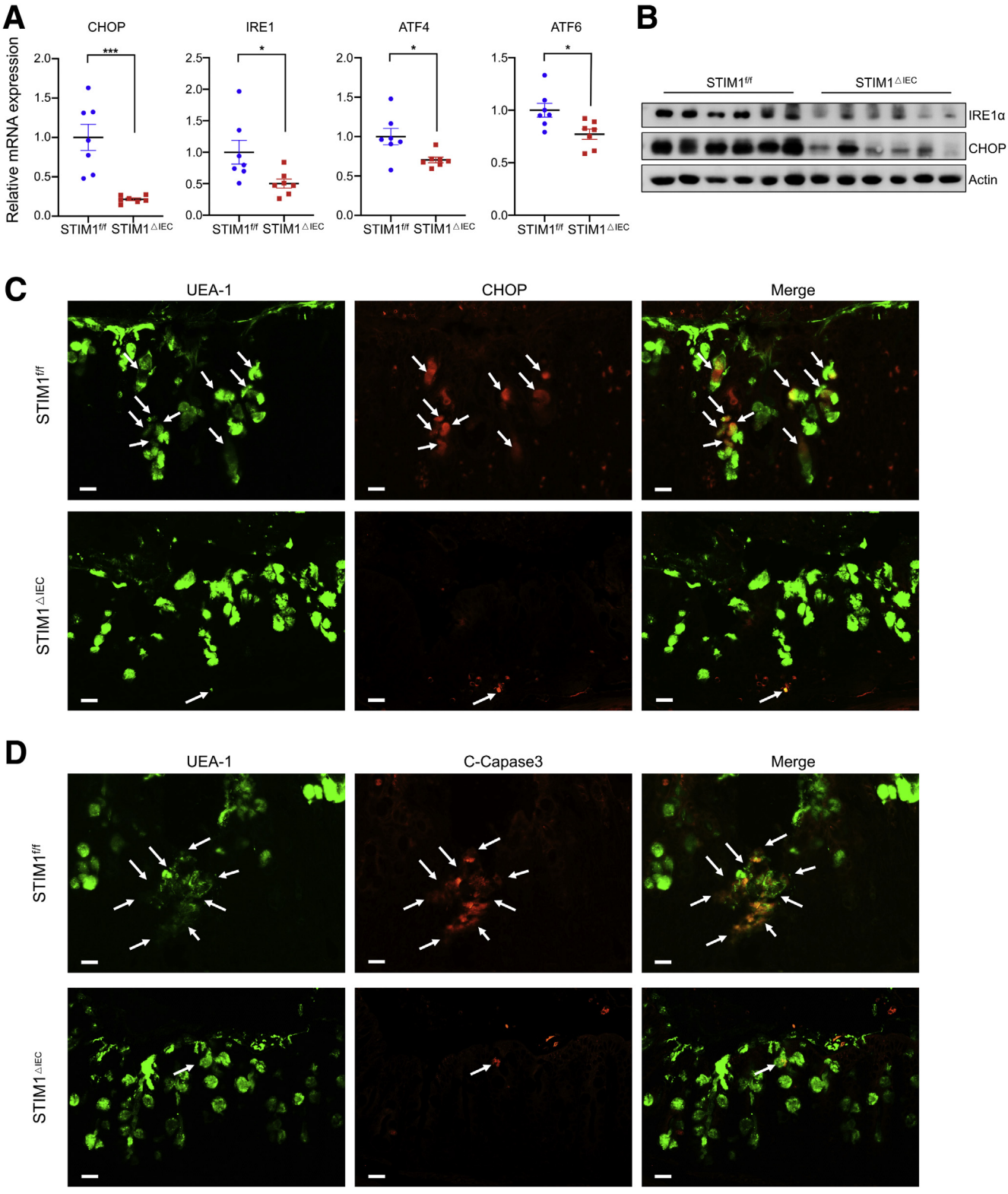

Figure 9. STIM1 deficiency in intestinal epithelium alleviates the ER stress and subsequent cell apoptosis of goblet cells. (*A*) Relative mRNA expression of the indicated genes related to ER stress in DSS-treated colon tissues on day 7 (n = 7 per group). (*B*) Analysis of protein levels of IRE1α and CHOP in DSS-treated colon tissues on day 7 (n = 6 per group). (*C*) DSS-treated colon sections on day 7 were stained for UEA-1 (green) and CHOP (red) to visualize ER stress in goblet cells (n = 3 per group). *Scale bars*: 20 μm. *Arrows* indicate goblet cells undergoing ER stress. (*D*) DSS-treated colon sections on day 7 were stained for UEA-1 (green) and C-Caspase 3 (red) to visualize apoptosis in goblet cells (n = 3 per group). *Scale bars*: 20 μm. *Arrows* indicate goblet cells undergoing apoptosis. Results are presented as the means ± SEM. ***$P < .001$; *$P < .05$.

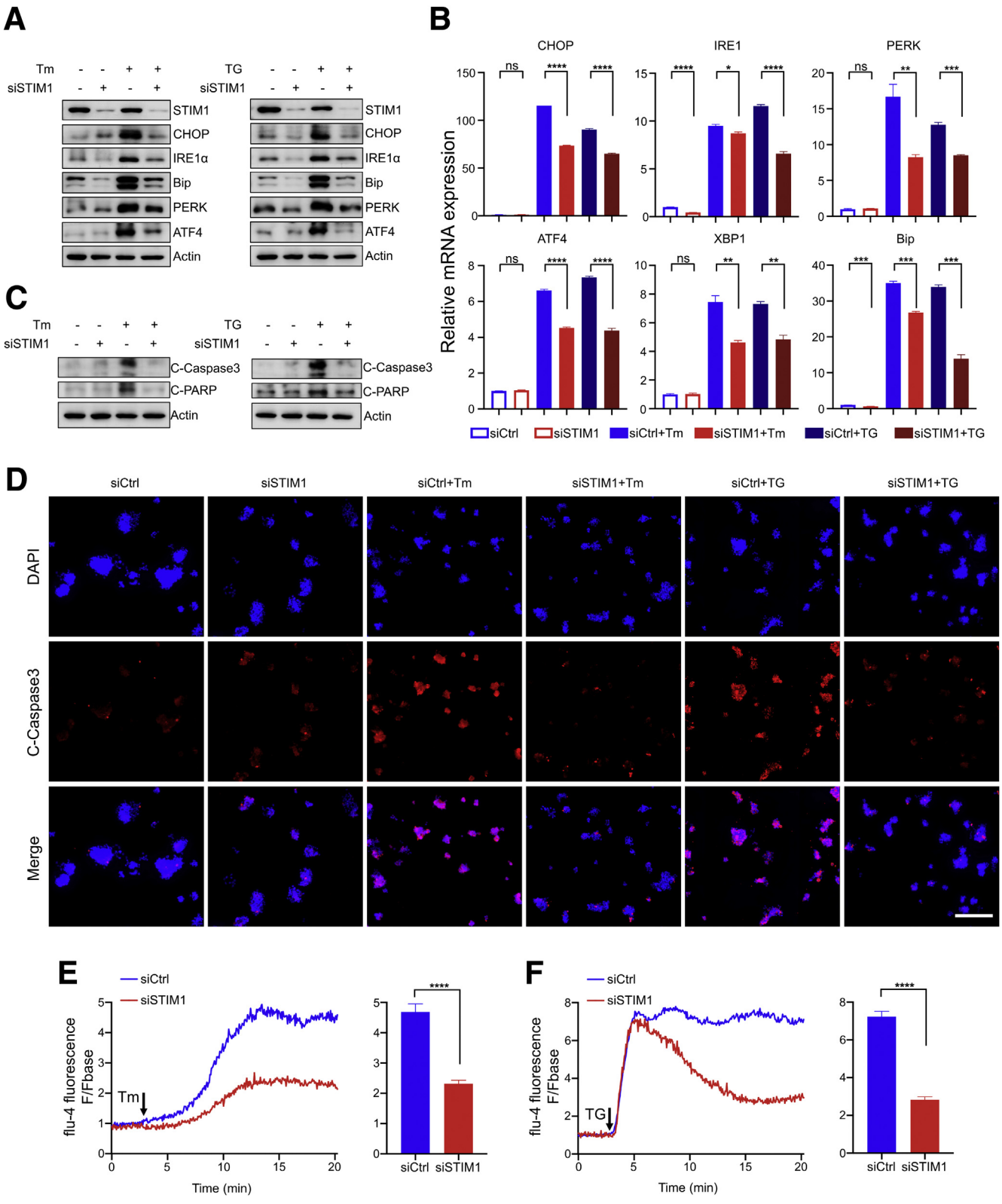

Figure 10. STIM1 knockdown in LS174T cells alleviates ER stress and prolonged ER stress–induced apoptosis by reducing Ca^{2+} overload. LS174T cells were treated with 10 μg/mL Tm or 5 μmol/L TG for 6 hours, 12 hours, or 24 hours with or without STIM1 knockdown. (*A*) ER stress was examined by WB at 12 hours. (*B*) ER stress was quantified by qPCR at 6 hours. (*C* and *D*) Apoptosis was examined by WB and immunostaining for C-Caspase 3 at 24 hours. *Scale bars*: 200 μm. (*E*) Tm- or (*F*) TG-induced intracellular Ca^{2+} concentrations were measured by Fluo-4 AM in 20 minutes (*left*), and representative changes in intracellular Ca^{2+} fluorescence intensity at 15 minutes (*right*) in LS174T cells with or without STIM1 knockdown were shown (n = 40 cells per group). Results are presented as the means ± SEM. ****$P < .0001$, ***$P < .001$, **$P < .01$, and *$P < .05$; NS at $P > .05$. DAPI, 4′,6-diamidino-2-phenylindole; F/Fbase, Ca^{2+} fluorescence intensity / base of Ca^{2+} fluorescence intensity; siCtrl, siRNA-Control; siSTIM1, siRNA-STIM1.

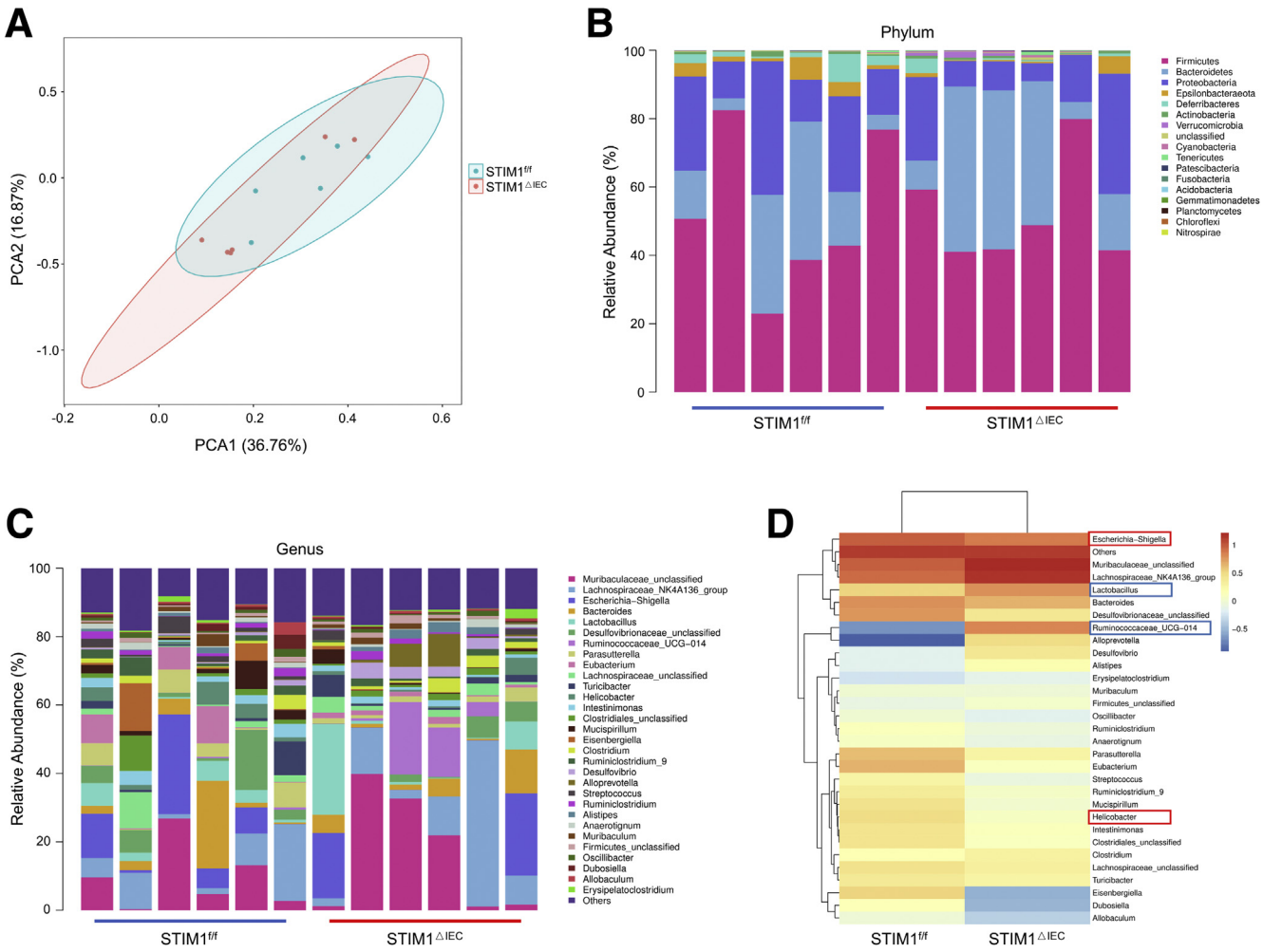

Figure 11. Abundance varied slightly between STIM1$^{\Delta IEC}$ and STIM1$^{f/f}$ mice. According to the results of 16S sequencing on day 7 of DSS administration (n = 6 per group), β-diversity was assessed by (*A*) principal component analysis (PCA). (*B*) Phylum diversity and (*C*) genus diversity are indicated by stacked bar charts. (*D*) Genus abundance is shown by a heatmap, indicating pathogenic microbiota in a *red frame* and beneficial bacterial species in a *blue frame*.

recovery. As anticipated, STIM1$^{f/f}$ mice did not recover to 95% of normal body weight throughout the convalescence (Figure 13*A*). Although colon length and the mRNA levels of inflammatory cytokines (except for IL1β) were similar between STIM1$^{\Delta IEC}$ and STIM1$^{f/f}$ mice (Figure 13*B* and *C*), histopathology showed that STIM1$^{f/f}$ mice suffered chronic inflammation manifested as ulceration, inflammatory cell infiltration, and partial loss of epithelium structure, while the epithelium of STIM1$^{\Delta IEC}$ mice almost recovered to normal (Figure 13*D* and *E*).

Next, we administered STIM1$^{\Delta IEC}$ and STIM1$^{f/f}$ mice azoxymethane followed by 3 cycles of DSS to sustain chronic inflammation and induce CAC. STIM1$^{\Delta IEC}$ mice showed decreased body weight loss (Figure 14*A*), accompanied by significantly higher survival rates and longer colon lengths (Figure 14*B* and *C*), indicating the inhibition of recurring colitis in STIM1$^{\Delta IEC}$ mice. Statistical analysis of tumors in the colon showed that STIM1$^{\Delta IEC}$ mice showed decreased numbers and sizes of tumors, and the tumor loads were significantly lower than those of STIM1$^{f/f}$ mice (tumors per mouse: 5.889 vs 9.056; large tumors ($\geq$3 mm) per mouse: 2.833 vs 4.278) (Figure 14*D*–*G*). Furthermore, histopathologic images showed that STIM1$^{\Delta IEC}$ mice had low-grade tumor dysplasia with almost normal adjacent mucosa, in contrast to STIM1$^{f/f}$ mice, which showed high-level dysplasia with massive mucosal hyperplasia (Figure 14*H* and *I*).

Overall, these results indicate that STIM1 is essential for the tumorigenesis of CAC by promoting acute and chronic inflammation.

Discussion

STIM1 has been confirmed to promote the formation of colorectal cancer.[23,42] As the initial stage of CAC, IBD patients have shown increased STIM1-mediated SOCE in lamina propria, and STIM1 also has been shown to be essential for T-cell–mediated immunoinflammatory diseases in mouse models.[26–29] However, the specific mechanisms by which intestinal STIM1 regulates the development of IBD

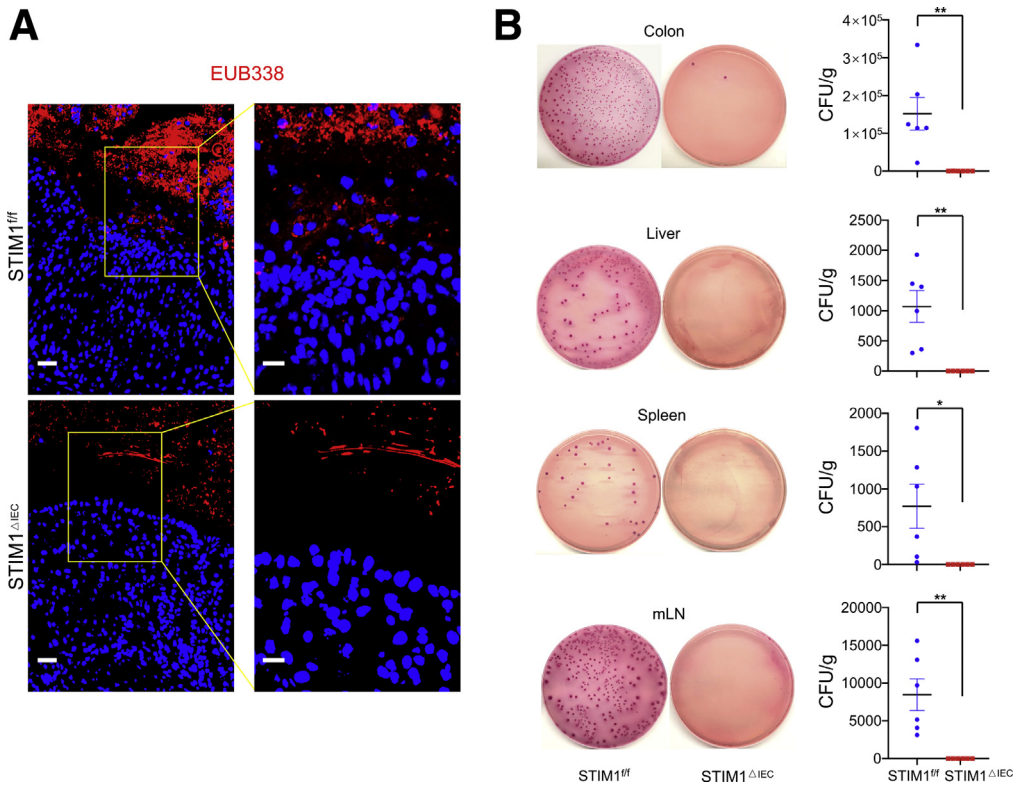

Figure 12. STIM1 deficiency in intestinal epithelium protects the intestinal epithelium against stimulation by commensal bacteria. (*A*) In situ EUB338 DNA probe hybridization of colon sections on day 7 of DSS administration, commensal bacteria are shown in red, nuclei are shown in blue (n = 5 per group). *Scale bars*: 20 μm, *boxed pullout*: 10 μm. (*B*) On day 7 of DSS administration, pathogenic bacterial translocation from intestinal lumina to colon tissues, liver, spleen, and mesenteric lymph nodes, as indicated by MacConkey agar plates (n = 6 per group). Data are presented as the means ± SEM. $^{**}P < .01$ and $^{*}P < .05$. CFU, colony-forming unit.

still are unclear. Here, we found that STIM1 was highly expressed in the inflammatory intestine of IBD patients. To investigate the role of intestinal epithelial STIM1 in IBD, we generated STIM1$^{\Delta IEC}$ mice with specific STIM1 deficiency in intestinal epithelium and discovered previously unknown roles of STIM1 in the regulation of mucosal inflammation, mucus barrier, and goblet cell ER stress.

The intestinal epithelia with active inflammation in IBD patients show ER stress signals.[19] Studies have confirmed that ER stress in IECs is the cause of intestinal inflammation, and high ER stress in IECs with high secretory activity could directly initiate and promote intestinal inflammation.[22] The expression levels of ER stress signals were decreased significantly in STIM1$^{\Delta IEC}$ mouse intestines, indicating that activated ER stress may be the major mechanism by which STIM1 promotes colitis. The colonic mucus layer is formed by large and complex mucins produced by goblet cells, among which MUC2 is the most essential. This function of goblet cells makes it susceptible to protein misfolding induced by environmental stimulation, including DSS treatment, and the accumulation of misfolded and aberrantly assembled MUC2 can cause ER stress in goblet cells.[19–21] Our studies indicated that the ER stress of goblet cells in STIM1$^{\Delta IEC}$ mice was decreased during colitis. Disturbances of ER–Ca^{2+} homeostasis induce ER stress and consequent cell apoptosis.[35,43] As the major component of SOCE, STIM1 is involved in the maintenance of Ca^{2+} homeostasis and has been confirmed to play complicated roles in ER stress. In our study, STIM1 deficiency in intestinal epithelium was first observed to ameliorate goblet cell ER stress. In addition, in STIM1-silenced LS174T cells, the induction of ER stress with Tm or TG was reduced by attenuating Ca^{2+} overload (Figure 10).

The prolonged stimulation of ER stressors can result in irremediable ER stress, activate the terminal unfolded protein response, and trigger caspase-dependent apoptosis.[44] Previous evidence has shown that irremediable ER stress–induced massive goblet cell loss is the cause of thinner and permeable mucus; furthermore, goblet cell loss is the defining feature of IBD patients and murine colitis.[45–48] A defective mucus barrier cannot effectively protect the intestine from various environmental stimuli. Mice with misfolded MUC2 in goblet cells lack mature MUC2 and cannot produce mucus, which lead to spontaneous colitis.[11] Mice with impaired secretory function of goblet cells also showed defective mucus, suffered mild proinflammation of the intestine, and were more susceptible to DSS-induced colitis.[12,13] In STIM1$^{\Delta IEC}$ mice, prolonged ER stress–induced goblet cell apoptosis and loss was inhibited, which ensured the normal production of MUC2 by goblet cells and the maintenance of the integrated inner mucus layer during colitis (Figure 7). In summary, the integrated mucus barrier protected STIM1$^{\Delta IEC}$ mice from DSS-induced colitis, suggesting a potential therapy for IBD by ameliorating ER stress in goblet cells to maintain an integrated mucus layer.

The outer mucus layer acts as a natural habitat and food source for commensal bacteria, of which the mucin

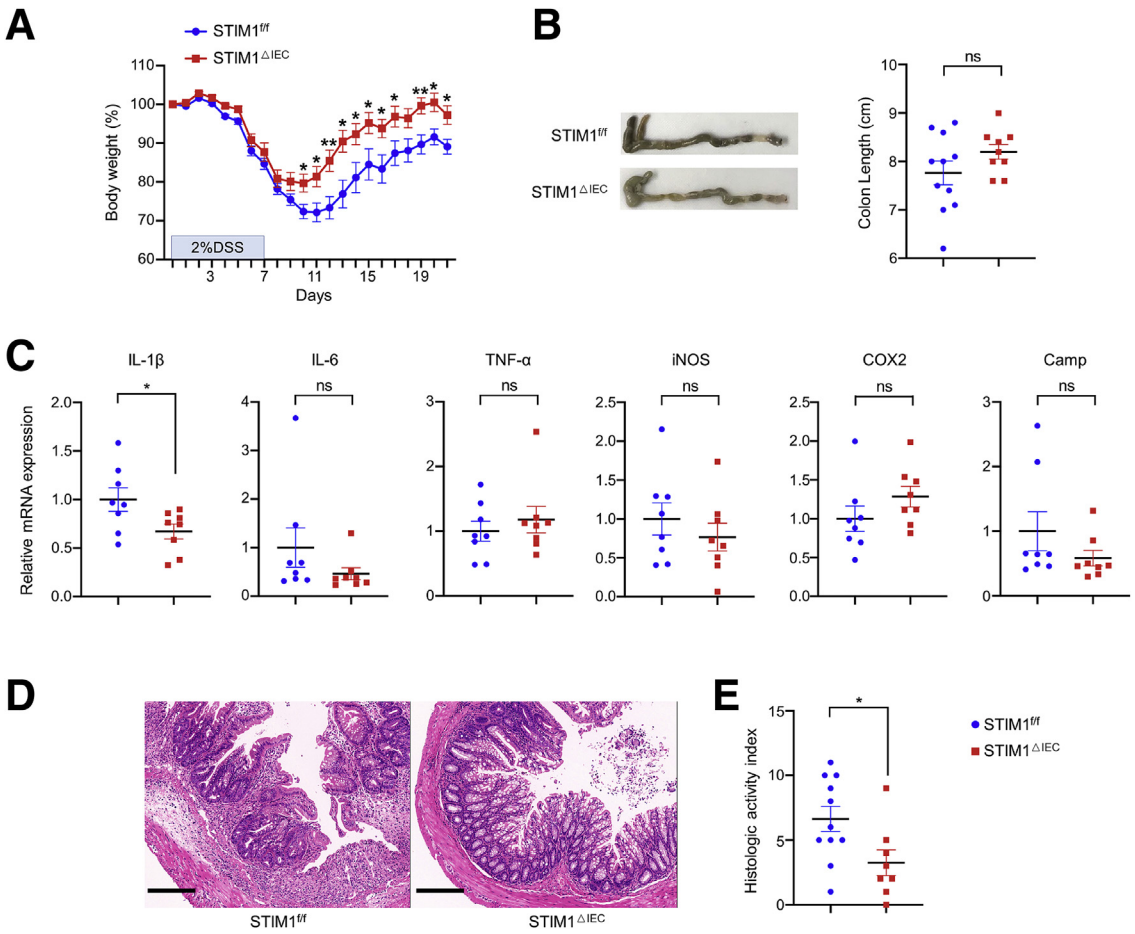

Figure 13. STIM1 deficiency in intestinal epithelium promotes recovery from colitis. (*A*) Percentage change in body weight during DSS-induced colitis followed by 14 days of convalescence (n = 13–17 per group). (*B*) Colon lengths on day 21 (n = 9–11 per group). (*C*) Relative mRNA expression of inflammatory cytokines in colon tissues on day 21 (n = 8 per group). (*D* and *E*) Representative H&E staining of colon sections and histologic activity index on day 21 (n = 8–11 per group). *Scale bars*: 200 μm. Data are presented as the means ± SEM. $^{**}P < .01$, $^{*}P < .05$; NS at $P > .05$. COX2, cyclooxygenase 2; iNOS, inducible nitric oxide synthase.

components can interact with the bacterial community.[49] Perturbation of genetic and environmental factors on bacterial community affects mucus glycosylation and promotes the development of intestinal inflammation.[1,39] However, in our study, although the mucus in STIM1$^{\Delta IEC}$ mice is rich as a consequence of decreased goblet cell loss, the alteration of bacterial community showed no statistical difference. The bacterial community of STIM1$^{\Delta IEC}$ mice had only slight differences at the genus level, including the contraction of pathogenic bacteria and the expansion of beneficial bacteria. Because the bacterial changes were not statistically significant, and the bacteria in STIM1$^{\Delta IEC}$ mice were completely prevented from contacting intestinal epithelium, we determined that the slight alteration in commensal bacteria was a consequence, but not the cause, of alleviated colitis in STIM1$^{\Delta IEC}$ mice. Interestingly, Ahuja et al[50] found that mice lacking acinar ORAI1 showed impaired antimicrobial pancreatic secretion, ultimately causing bacterial outgrowth and inflammation in the intestine. Patients with ORAI1 mutations also showed immunodeficiency and increased infections of viral, bacterial, and fungal pathogens.[51] Because STIM1 deficiency in intestinal epithelium alleviates colitis mainly by affecting the function and loss of goblet cells, we speculated that it was the discrepancy in cell-specific results that caused our contrary results to those reported previously.

In patients and mouse models of IBD, the defective mucus barrier allows massive numbers of bacteria to penetrate and reach the epithelium to activate the immune system.[6] Mononuclear phagocytes mediate the initiation of proinflammatory effects. Through the toll like receptor - myeloid differentiation primary response 88 (TLR–MyD88) signaling pathway, TLRs recognize bacterial molecules and promote immune responses to produce inflammatory cytokines, including IL1, IL23, IL6, and IL10, which are essential in inducing T-cell responses.[1] Moreover, the increase of interferon-γ and TNF-α can disrupt epithelial cell junctions to induce epithelial barrier dysfunction, which further increase epithelial permeability and enhance bacteria-induced immune response.[5] sIgA is

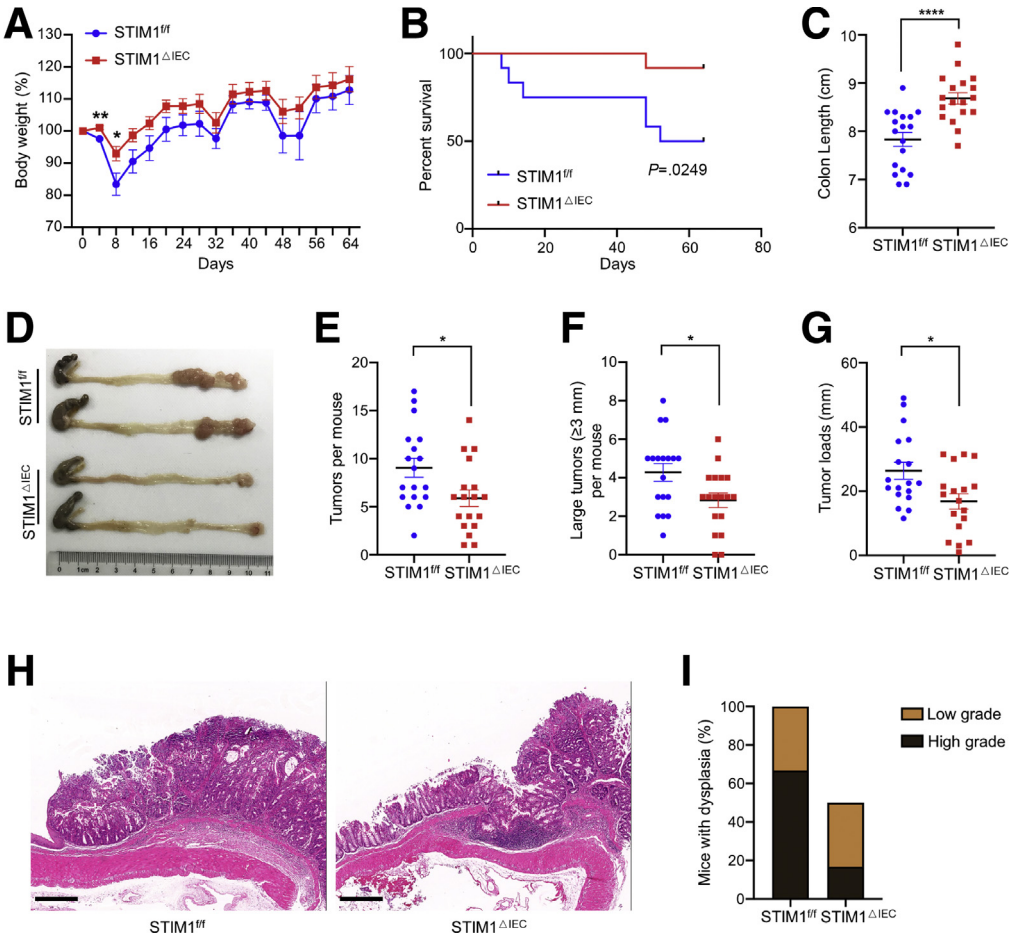

Figure 14. STIM1 deficiency in intestinal epithelium renders mice less susceptible to CAC. (*A*) Percentage change in body weight and (*B*) Kaplan–Meier survival curves throughout azoxymethane/DSS-induced CAC (n = 12 per group). (*C*) Analysis of colon length in mice with colorectal tumors (n = 18 per group). (*D*) Representative images of colonic tumors. (*E*) Number of colon tumors per mouse (n = 18 per group). (*F*) Number of large tumors (diameter, ≥3 mm) per mouse (n = 18 per group). (*G*) Tumor loads indicated by the sum of tumor diameters per mouse (n = 18 per group). (*H*) Representative H&E-stained colon sections and tumor morphology (n = 6 per group). *Scale bars*: 400 μm. (*I*) Percentages of mice with tumor dysplasia. Kaplan–Meier survival curves were analyzed by the log-rank test, while other differences were verified using a 2-tailed Student *t* test. Data are depicted as the means ± SEM. ****$P < .0001$, **$P < .01$, and *$P < .05$.

generated by plasma cells in lymphoid follicles and intestinal lamina propria in response to bacteria stimulation.[52] The integrated mucus layer protects STIM1$^{\Delta IEC}$ mice against bacterial stimulation, thereby decreasing the production of sIgA and inflammatory cytokines and preventing acute or chronic inflammation. Recurrently chronic mucosal inflammation stimulated by bacteria can lead to epithelial apoptosis and subsequent pathologic epithelial proliferation, which are known to be essential for the development of CAC. Therefore, it is not surprising that the number and size of tumors in STIM1$^{\Delta IEC}$ mice were decreased significantly (Figure 14), which further supports the previous evidence that commensal microbiota penetrating the defective mucus barrier contribute to the tumorigenesis of CAC.[8,9]

The precise mechanism by which STIM1 regulates ER stress of goblet cells needs further clarification. ER is the primary store of Ca^{2+}, steady ER–Ca^{2+} homeostasis can control intracellular Ca^{2+} homeostasis to ensure normal ER function, for example, protein glycosylation and protein folding in ER require Ca^{2+}-dependent calnexin and calreticulin.[53] ER–Ca^{2+} homeostasis is perturbed easily by ER stressors, and disturbed ER–Ca^{2+} homeostasis accompanied by intracellular Ca^{2+} overload can elicit protein misfolding, which results in ER stress.[35] The prolonged intracellular Ca^{2+} overload further aggravates ER stress and causes cell death.[54] STIM1 is the activator of SOCE to supply intracellular Ca^{2+}, and its knockdown has been shown to protect cells against ER stress and apoptosis through abrogating cytoplasmic Ca^{2+} overload induced by stressors.[55,56] Our study confirmed that STIM1 deficiency reduced intracellular Ca^{2+} overload induced by ER stressors in goblet cells, leading to a striking decrease in ER stress and apoptosis of goblet cells (Figure 15). Based on these results, inhibiting stressor-induced Ca^{2+} overload to maintain ER–Ca^{2+} homeostasis may be a potential therapeutic option to reduce ER stress and apoptosis of goblet cells during colitis.

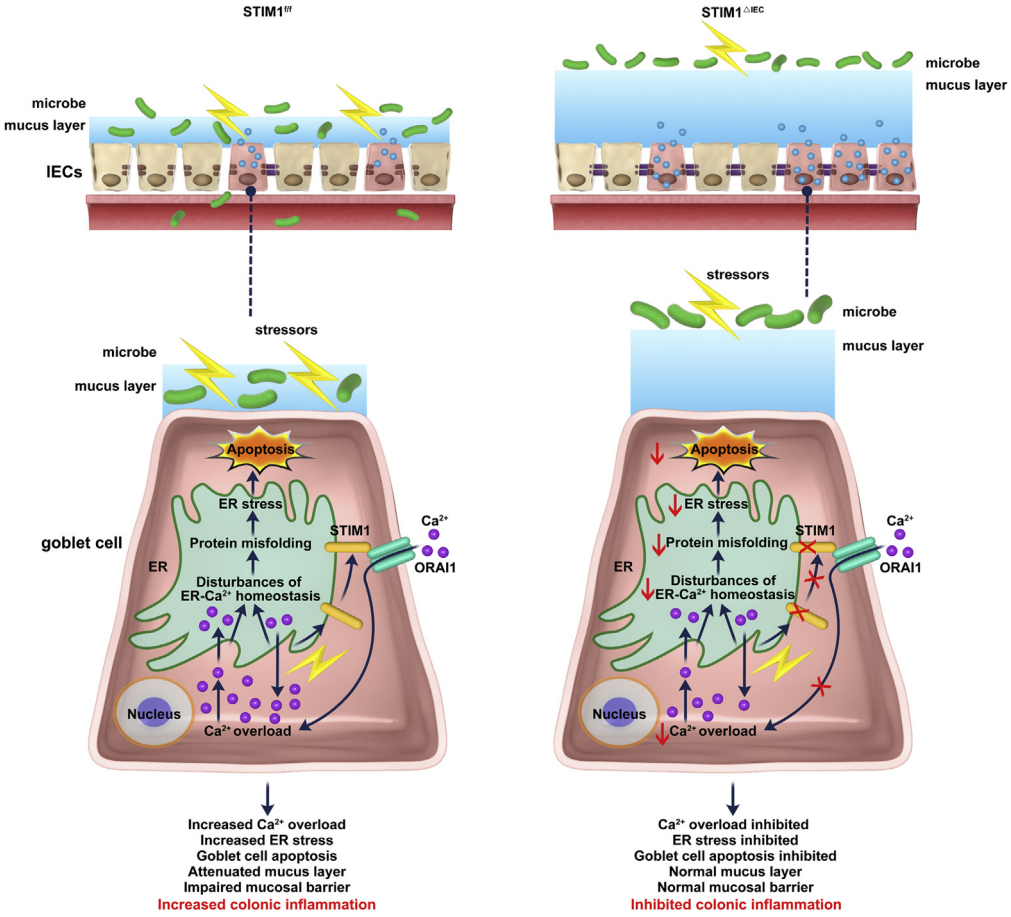

Figure 15. During DSS treatment, infinitesimal bacteria penetrate inner mucus layer before the inflammation reactions and stimulate goblet cells to generate and secret mucus. The stimulation of bacteria is determined as ER stressors and can disturb ER-Ca^{2+} homeostasis accompanied by intracellular Ca^{2+} overload and elicit protein misfolding, resulting in ER stress and subsequent apoptosis. Goblet cell depletion diminishes mucus synthesis, defective mucus layer would allow massive bacteria to reach to intestinal epithelium, driving further impairment to mucosal barrier and activating immune responses to trigger mucosal inflammation and tumorigenesis. STIM1 deficiency in intestinal epithelium alleviates the disturbance of Ca^{2+} homeostasis to inhibit ER stress and subsequent depletion of goblet cells, maintaining the integrity of mucus barrier, therefore alleviating colitis and tumorigenesis in mice.

In conclusion, our results show that STIM1 is overexpressed in LP and IECs of IBD patients, which further confirms the previous theory that STIM1 is involved in immunoinflammatory diseases. Meanwhile, our study provides evidence that STIM1 in intestinal epithelium regulates ER stress and subsequent apoptosis of colonic goblet cells, providing a new perspective for the mechanism of STIM1 promoting colitis and colorectal cancer. Developing inhibitors that specifically target STIM1 in intestinal epithelium would be a potential treatment strategy for IBD and CAC.

Materials and Methods

Patients

Human intestinal inflammatory tissues and matched-adjacent normal tissues were collected from IBD patients at the Department of Pathology, Sir Run Run Shaw Hospital, Zhejiang University (ethics approval 20210125-30).

LS174T Cell Culture and Treatment

LS174T colon carcinoma cells, which were differentiated by goblet cells, were purchased from the Cell Bank of the Chinese Academy of Science and maintained in Dulbecco's modified Eagle medium (#MA0212; Meilunbio, Dalian, China) with 10% fetal bovine serum (FBS) (#NFBS-2500A; Noverse, Uruguay, South America) at 37°C and 5% CO_2. LS174T cells were treated with tunicamycin (#HY-A0098; MCE, South Brunswick Township, NJ) at 10 μg/mL, and thapsigargin (#T9033; Sigma-Aldrich, St. Louis, MO) at 5 μmol/L for 6 or 12 hours. The small interfering RNA sequence against human STIM1 is 5'-GGGAA-GACCTCAATTACCA-3'.

Mice

Mice carrying STIM1 floxed alleles were generated as previously described,[25] and they were crossed with Villin-*Cre* mice (purchased from Shanghai Model Organisms, Shanghai, China) to obtain $STIM1^{\Delta IEC}$ mice. All mice were

bred and housed in specific pathogen-free conditions, and sex- and age-matched mice (age, 8–10 wk; weight, 23–25 g) were used for each experiment (ethics approval ZJU2015-220-01).

Experimental Colitis and CAC

To induce acute colitis, mice were administered 2% DSS (molecular weight, 36,000–50,000 Daltons; MP Biomedicals, Irvine, CA) in drinking water for 7 days, followed by regular drinking water for 3–4 days until the mice lost more than 25% of their body weight. The body weight and disease activity index (including weight loss, stool consistency, and the presence of fecal blood) were recorded every day until the mice were killed.

To induce CAC, mice were injected with azoxymethane (10 mg/kg; MP Biomedicals) intraperitoneally, and after 7 days of regular water they were administered 3 cycles of 2% DSS in drinking water for 6 days, followed by regular water for 15 days.

Intestinal Permeability

Four hours before the mice were killed, the mice were orally gavaged with FITC–dextran (0.6 mg/kg body weight; Sigma-Aldrich), and blood samples were collected via cardiac puncture. After clotting and centrifuging, the supernatant of the blood sample was analyzed at 485/535 nm on a Synergy H4 Hybrid Reader (Biotek, Winooski, VT).

Bacterial Translocation

After the mice were killed, whole mouse mLNs, spleens, and livers were removed, weighed, and collected in 1 mL sterile phosphate-buffered saline (PBS) with EDTA-free protease inhibitor cocktail. Colons were opened longitudinally and washed in sterile PBS several times to completely remove stool. Then, 0.1 g colon tissue was removed and collected in 0.9 mL sterile PBS with EDTA-free protease inhibitor cocktail. All tissues were homogenized in a bead miller (JXFSTPRP-CL, Jing xin, Shanghai, China) for 2 minutes at 4°C. Then, 200 uL tissue homogenate was plated on MacConkey agar plates (#M8560; Solarbio, Beijing, China) and incubated at 37°C and 5% CO_2 for 48 hours, and the number of bacterial colonies on the plates was counted and normalized to the tissue weight (per gram).

Cytokine Determination

The supernatants of blood and tissue homogenates were analyzed with enzyme-linked immunosorbent assay kits according to the manufacturer's recommendations to detect the levels of IL6, TNF-α (Invitrogen, Carlsbad, CA), and sIgA (MultiSciences, Hangzhou, China).

Histopathology, Immunostaining, and Fluorescence In Situ Hybridization

Colon sections (approximately 2-cm long) were fixed in neutral-buffered formalin (#G1101; Servicebio, Wuhan, China) overnight at 4°C, and embedded in paraffin, and then 5-um–thick tissue sections were stained with H&E (Servicebio) for histopathology. The histologic activity index of colon sections was scored blindly based on the extent and severity of the inflammation, ulceration, and hyperplasia of mucosa as previously described.[57]

For immunohistochemistry, colon tissue sections were stained with STIM1 (#5668; CST, Danvers, MA,), Cdh1 (#3195; CST), and occludin (#71-1500; Thermo Fisher, Waltham, MA) according to the manufacturer's recommendations. Immunohistochemical scores of STIM1 were assigned as previously described[58]: 3, intense and granular cytoplasmic staining; 2, moderate and smooth cytoplasmic staining; 1, faint and barely discernable cytoplasmic staining; and 0, no staining. The proportion of positive cells in tissue sections was determined using Image-Pro Plus 6.0 (Media Cybernetics, Rockville, MD), and 4–5 regions of interest were assessed per mouse.

For immunofluorescence, tissue slides were stained with CD45 (#40763; Abcam, Waltham, MA), EpCAM (#A1177; Abclonal, Wuhan, China), FITC-conjugated UEA-1 (#L9006; Sigma), CHOP (#2895; CST), and C-Caspase 3 (#9664; CST).

To detect whether the bacteria were in contact with intestinal epithelium, an EUB338 DNA probe (5′-GCTGCCTCCCGTAGGAGT-3′; Servicebio) was used for fluorescence in situ hybridization.

Goblet Cells and Mucus Layer Preservation Ex Vivo

The terminal colons with stool were excised and immediately submerged in Carnoy fixative at 4°C for 2 hours and then placed into 100% ethanol. Fixed colon tissues were embedded in paraffin and stained with PAS or Alcian blue/PAS. The number of goblet cells and the thickness of the inner mucus layer were measured by Image-Pro Plus 6.0, 4–5 regions of interest were measured per mouse and the mean was calculated.

PAS Assay

A total of 100 μL colon tissue homogenate supernatant was prepared as described earlier, and incubated with 200 μL of 0.1% periodic acid (0.1 g/100 mL; Solarbio) at room temperature for 2 hours. Then, 200 μL Schiff reagent (Solarbio) was added and incubated for 30 minutes at room temperature. The resulting mixture was measured at 555 nm and the PAS optical density value was normalized to that of $STIM1^{f/f}$ mice.

Isolation of IECs

Colons from experimental mice were freshly isolated, opened longitudinally, and washed using ice-cold sterile PBS several times to completely remove stool. Clean colon tissues were cut into 2-mm segments and incubated in Hank's balanced salt solution (HBSS) (without calcium chloride, magnesium sulfate, or sodium bicarbonate; Sigma-Aldrich) with 30 mmol/L EDTA (Sigma-Aldrich) and 1.5 mmol/L dithiothreitol (Sigma-Aldrich) at 4°C for 20 minutes to remove mucus. Then, the colon pieces were washed in HBSS and incubated in HBSS with 30 mmol/L EDTA and 2% FBS in a shaker at 200

Table 1. Primer Sequences

Name	Sequences
Mouse GAPDH	F: TCACCACCATGGAGAAGGC R: GCTAAGCAGTTGGTGGTGCA
Mouse STIM1	F: TGAAGAGTCTACCGAAGCAGA R: AGGTGCTATGTTTCACTGTTGG
Mouse Chga	F: ATCCTCTCTATCCTGCGACAC R: GGGCTCTGGTTCTCAAACACT
Mouse Lyz1	F: AATGGATGGCTACCGTGGTGT R: TAGTCGGTGCTTCGGTCTC
Mouse Spdef	F: TTGCCTGCTACTGTTCCCAG R: CCAGGGTCTGCTGTGATGTT
Mouse NFATc1	F: TGCCTTTTGCGAGCAGTATCT R: CAGGCAAGGATGGGCTCATAT
Mouse NFATc2	F: GGATCCCCTCCAAGATATGG R: CCCCAGGAACTCCACAGTAG
Mouse NFATc3	F: TGACTTCTCCAGGTGGCTCT R: GAGAGTGGCAAGGAGATTGC
Mouse NFATc4	F: GAGGAGCCCCTACCAGACTC R: AGGGTCTTCATGGGGATAGG
Mouse IL6	F: GAGGATACCACTCCCAACAGACC R: AAGTGCATCATCGTTGTTCATACA
Mouse IL10	F: GGTTGCCAAGCCTTATCGGA R: ACCTGCTCCACTGCCTTGCT
Mouse IL1β	F: GCTGAAAGCTCTCCACCTCA R: AGGCCACAGGTATTTTGTCG
Mouse TNF-α	F: TACTGAACTTCGGGGTGATCGGTCC R: CAGCCTTGTCCCTTGAAGAGAACC
Mouse iNOS	F: CAGCTGGGCTGTACAAACCTT R: CATTGGAAGTGAAGCGTTTCG
Mouse cyclooxygenase 2	F: AAGGAACTCAGCACTGCATCC R: ACAGGGATTGGAACAGCAAGGA
Mouse Camp	F: CAGCCCTTTCGGTTCAAGAA R: CCCACCTTTGCGGAGAAGT
Mouse Cdh1	F: TCCTTGTTCGGCTATGTGTC R: GGCATGCACCTAAGAATCAG
Mouse occludin	F: TTGAAAGTCCACCTCCTTACAGA R: CCGGATAAAAAGAGTACGCTGG
Mouse ZO1	F: GCCGCTAAGAGCACAGCAA R: GCCCTCCTTTTAACACATCAGA
Mouse ZO2	F: ATGGGAGCAGTACACCGTGA R: TGACCACCCTGTCATTTTCTTG
Mouse ZO3	F: TCGGCATAGCTGTCTCTGGA R: GTTGGCTGTTTTGGTGCAGG
Mouse Cldn2	F: GGCTGTTAGGCACATCCAT R: TGGCACCAACATAGGAACTC
Mouse Cldn3	F: AAGCCGAATGGACAAAGAA R: CTGGCAAGTAGCTGCAGTG
Mouse Cldn7	F: AGGGTCTGCTCTGGTCCTT R: GTACGCAGCTTTGCTTTCA
Mouse Muc2	F: CCTGAAGACTGTCGTGCTGT R: GGGTAGGGTCACCTCCATCT
Mouse AGR2	F: CGGTGAGGGCAGACATCACTGGA R: CCGGTGCGCAGTTGGCTCTA
Mouse Atoh1	F: AAAGGAGGCTGGCAGCAA R: TGGTTCAGCCCGTGCAT
Mouse Klf4	F: AGGCACACCTGCGAACTCA R: CAGCCGTCCCAGTCACAGT

Table 1. Continued

Name	Sequences
Mouse Hes1	F: CCCCAGCCAGTGTCAACAC R: TGTGCTCAGAGGCCGTCTT
Mouse CHOP	F: AACAGAGGTCACACGCACAT R: TTCCTCCTCTTCCTCCTGGG
Mouse IRE1	F: GCCCAACGCACATGGCAGGA R: TACCCCTGAACGGCGGCTGA
Mouse ATF4	F: TGCTGTCTGCCGGTTTAAGT R: CTGCTGCCTCTAATACGCCA
Mouse ATF6	F: GGGCAGGGCCATTCTTGCTGA R: AGCCCCCGGGACAAACAGGT
Human actin	F: GAGCTACGAGCTGCCTGAC R: GGTAGTTTCGTGGATGCCACAG
Human CHOP	F: GCGCATGAAGGAGAAAGAAC R: CCAATTGTTCATGCTTGGTG
Human IRE1	F: GGACAGGCTCAATCAAATGG R: CGGTCAGGAGGTCAATAACA
Human PERK	F: CGATGAGACAGAGTTGCGAC R: TGCTTTCACGGTCTTGGTC
Human Bip	F: GCCTGTATTTCTAGACCTGCC R: TTCATCTTGCCAGCCAGTTG
Human ATF4	F: AGTTCGACTTGGATGCCCTG R: CCAACGTGGTCAGAAGGTCA
Human XBP1	F: GCTCAGACTGCCAGAGATCG R: GCGCTGTCTTAACTCCTGGT

AGR2, anterior gradient 2; ATF, activating transcription factor; Atoh1, atonal BHLH transcription factor 1; Chga, chromogranin A; Camp, cathelicidin antimicrobial peptide; F, forward; GAPDH, glyceraldehyde-3-phosphate dehydrogenase; Hes1, hes family BHLH transcription factor 1; iNOS, inducible nitric oxide synthase; Klf4, kruppel like factor 4; Lyz1, lysozyme 1; NFAT, nuclear factor of activated T Cells; R, reverse; Spdef, SAM pointed domain containing ETS transcription factor; XBP1, X-box binding protein 1.

rpm and 37°C for 60 minutes. The resulting supernatants contained IECs, and were collected for RNA extraction and Western blot.

16S Sequencing

After the mice were killed, the fresh colonic contents were collected from colitis mice, and DNA was extracted using the Stool DNA Kit (#D4015; Omega, Norcross, GA) according to the manufacturer's recommendations. Primers for 341F (5'-CCTACGGGNGGCWGCAG-3') and 805R (5'-GACTACHVGGGTATCTAATCC-3') were used to amplify the bacterial V3–V4 region of the 16S ribosomal RNA gene as previously described.[59] The amplicon libraries of samples were sequenced on an Illumina NovaSeq platform (San Diego, CA) according to the instructions provided by LC-Bio Technology (Hangzhou, China).

Scanning Electron Microscopy and Transmission Electron Microscopy

Fresh distal colon tissues of experimental mice were removed and fixed with 2.5% glutaraldehyde in phosphate buffer (0.1 mol/L, pH 7.0) overnight at 4°C. Fixed samples were washed 3 times in phosphate buffer for 15 minutes, followed by postfixation with 1% OsO_4 in phosphate buffer for 1–2 hours. After being washed 3 times in phosphate buffer, tissues were dehydrated through a graded series of ethanol. The dehydrated samples all were viewed using Hitachi model SU-8010 scanning electron microscopy or embedded in Spurr resin, sliced into ultrathin sections, stained, and observed with Hitachi model H-7650 transmission electron microscopy (Tokyo, Japan).

Measurement of Intracellular Calcium

LS174T cells seeded in 35-mm diameter, glass-bottom dishes (#D35-20-0-N; Cellvis, Mountin View, CA) were loaded with 5 μmol/L Flu-4/AM (#S1060; Beyotime, Shanghai, China) for 30 minutes in Dulbecco's modified Eagle medium with 10% FBS at room temperature. Then, cells were washed and immersed in HBSS (#C0218; Beyotime) with 2 mmol/L Ca^{2+}, and images were recorded and analyzed every 4 seconds at an excitation wavelength of 488 nm using the Leica Application Suite X confocal imaging system (Solms, Germany). Changes in intracellular Ca^{2+} fluorescence intensity (F) were normalized to base of Ca^{2+} fluorescence intensity (Fbase) and were presented as F/Fbase.

WB

Proteins were extracted from IECs, colon tissues, human tissues, and LS174T cells using RIPA lysis buffer (#MA0151; Meilunbio) with protease and phosphatase inhibitor

cocktails (Bimake, Houston, TX). Lysate samples were separated by 10% sodium dodecyl sulfate–polyacrylamide gels, transferred to polyvinylidene fluoride membranes, and incubated with the following antibodies: *Actin* (#8457, CST), *STIM1* (#5668; CST), *Cdh1* (#3195; CST), *occludin* (#71-1500; Thermo Fisher), *ZO1* (#96587; Abcam), *ATF4* (#11815; CST), *Bip* (#3177; CST), *CHOP* (#2895; CST), *PERK* (#5683; CST), *IRE1α* (#3294; CST), and *C-PARP* (#9546; CST). After being incubated with anti-rabbit/mouse horseradish-peroxidase antibodies, signals were analyzed by enhanced chemiluminescence (Amersham Imager 600, GE, Boston, MA).

RNA Sequencing, Extraction, Reverse Transcription, and qPCR

Total RNA of colon tissues collected from experimental mice were extracted by Total RNA Extraction Reagent (#R401-01-AA; Vazyme, Nanjing, China). The mRNA was purified by oligodeoxythymidylate (oligo(dT))-attached magnetic beads, and then the purified mRNA was fragmented into small pieces to amplify and generate DNA nanoballs with more than 300 copies of 1 molecule. The DNA nanoballs were loaded into the patterned nanoarray, and paired-end 100 base reads were generated using the BGIseq500 platform (BGI, Shenzhen, China).

Total RNA of IECs, mouse tissues (colon, spleen, and thymus), and LS174T cells was extracted by the Total RNA Extraction Reagent, and reverse transcription was performed using the HiScript II 1st-Strand complementary DNA Synthesis Kit (#R312-02; Vazyme) according to the manufacturer's instructions. qPCR was performed using MagicSYBR Mixture (#CW3008M; CWBIO). Glyceraldehyde-3-phosphate dehydrogenase and actin were used for normalization of mouse samples and human samples, respectively. The primer sequences used to analyze the targeted gene expression are shown in Table 1.

Statistical Analysis

The data are presented as the means ± SEM. All statistical analyses were performed using GraphPad Prism (GraphPad Software, San Diego, CA). The Student t test (unpaired or paired Student t test) and 1-way analysis of variance were used for comparisons between 2 groups or multiple groups, respectively. Survival analysis was performed by the log-rank (Mantel–Cox) test. Statistical significance was considered to be $^{****}P < .0001$; $^{***}P < .001$; $^{**}P < .01$; $^{*}P < .05$; and NS at $P > .05$.

References

1. Pickard JM, Zeng MY, Caruso R, Núñez G. Gut microbiota: role in pathogen colonization, immune responses, and inflammatory disease. Immunol Rev 2017; 279:70–89.
2. Odenwald MA, Turner JR. The intestinal epithelial barrier: a therapeutic target? Nat Rev Gastroenterol Hepatol 2017;14:9–21.
3. Pelaseyed T, Bergström JH, Gustafsson JK, Ermund A, Birchenough GM, Schütte A, van der Post S, Svensson F, Rodríguez-Piñeiro AM, Nyström EE, Wising C, Johansson ME, Hansson GC. The mucus and mucins of the goblet cells and enterocytes provide the first defense line of the gastrointestinal tract and interact with the immune system. Immunol Rev 2014; 260:8–20.
4. Yu LC. Microbiota dysbiosis and barrier dysfunction in inflammatory bowel disease and colorectal cancers: exploring a common ground hypothesis. J Biomed Sci 2018;25:79.
5. Wang F, Graham WV, Wang Y, Witkowski ED, Schwarz BT, Turner JR. Interferon-gamma and tumor necrosis factor-alpha synergize to induce intestinal epithelial barrier dysfunction by up-regulating myosin light chain kinase expression. Am J Pathol 2005; 166:409–419.
6. Johansson ME, Gustafsson JK, Holmén-Larsson J, Jabbar KS, Xia L, Xu H, Ghishan FK, Carvalho FA, Gewirtz AT, Sjövall H, Hansson GC. Bacteria penetrate the normally impenetrable inner colon mucus layer in both murine colitis models and patients with ulcerative colitis. Gut 2014;63:281–291.
7. Johansson ME, Gustafsson JK, Sjöberg KE, Petersson J, Holm L, Sjövall H, Hansson GC. Bacteria penetrate the inner mucus layer before inflammation in the dextran sulfate colitis model. PLoS One 2010;5:e12238.
8. Neurath MF. Targeting immune cell circuits and trafficking in inflammatory bowel disease. Nat Immunol 2019;20:970–979.
9. Velcich A, Yang W, Heyer J, Fragale A, Nicholas C, Viani S, Kucherlapati R, Lipkin M, Yang K, Augenlicht L. Colorectal cancer in mice genetically deficient in the mucin Muc2. Science 2002;295:1726–1729.
10. Maloy KJ, Powrie F. Intestinal homeostasis and its breakdown in inflammatory bowel disease. Nature 2011; 474:298–306.
11. Van der Sluis M, De Koning BA, De Bruijn AC, Velcich A, Meijerink JP, Van Goudoever JB, Büller HA, Dekker J, Van Seuningen I, Renes IB, Einerhand AW. Muc2-deficient mice spontaneously develop colitis, indicating that MUC2 is critical for colonic protection. Gastroenterology 2006;131:117–129.
12. Cornick S, Kumar M, Moreau F, Gaisano H, Chadee K. VAMP8-mediated MUC2 mucin exocytosis from colonic goblet cells maintains innate intestinal homeostasis. Nat Commun 2019;10:4306.
13. Lian Q, Yan S, Yin Q, Yan C, Zheng W, Gu W, Zhao X, Fan W, Li X, Ma L, Ling Z, Zhang Y, Liu J, Li J, Sun B. TRIM34 attenuates colon inflammation and tumorigenesis by sustaining barrier integrity. Cell Mol Immunol 2021;18:350–362.
14. McCool DJ, Okada Y, Forstner JF, Forstner GG. Roles of calreticulin and calnexin during mucin synthesis in LS180 and HT29/A1 human colonic adenocarcinoma cells. Biochem J 1999;341:593–600.
15. Corbett EF, Michalak M. Calcium, a signaling molecule in the endoplasmic reticulum? Trends Biochem Sci 2000; 25:307–311.
16. Vassilakos A, Michalak M, Lehrman MA, Williams DB. Oligosaccharide binding characteristics of the molecular

chaperones calnexin and calreticulin. Biochemistry 1998; 37:3480–3490.
17. Tanikawa Y, Kanemura S, Ito D, Lin Y, Matsusaki M, Kuroki K, Yamaguchi H, Maenaka K, Lee YH, Inaba K, Okumura M. Ca(2+) Regulates ERp57-calnexin complex formation. Molecules 2021;26:2853.
18. Di Jeso B, Ulianich L, Pacifico F, Leonardi A, Vito P, Consiglio E, Formisano S, Arvan P. Folding of thyroglobulin in the calnexin/calreticulin pathway and its alteration by loss of Ca2+ from the endoplasmic reticulum. Biochem J 2003;370:449–458.
19. Heazlewood CK, Cook MC, Eri R, Price GR, Tauro SB, Taupin D, Thornton DJ, Png CW, Crockford TL, Cornall RJ, Adams R, Kato M, Nelms KA, Hong NA, Florin TH, Goodnow CC, McGuckin MA. Aberrant mucin assembly in mice causes endoplasmic reticulum stress and spontaneous inflammation resembling ulcerative colitis. PLoS Med 2008;5:e54.
20. Coleman OI, Haller D. ER stress and the UPR in shaping intestinal tissue homeostasis and immunity. Front Immunol 2019;10:2825.
21. Tawiah A, Cornick S, Moreau F, Gorman H, Kumar M, Tiwari S, Chadee K. High MUC2 mucin expression and misfolding induce cellular stress, reactive oxygen production, and apoptosis in goblet cells. Am J Pathol 2018; 188:1354–1373.
22. Kaser A, Lee AH, Franke A, Glickman JN, Zeissig S, Tilg H, Nieuwenhuis EE, Higgins DE, Schreiber S, Glimcher LH, Blumberg RS. XBP1 links ER stress to intestinal inflammation and confers genetic risk for human inflammatory bowel disease. Cell 2008;134:743–756.
23. Wang JY, Sun J, Huang MY, Wang YS, Hou MF, Sun Y, He H, Krishna N, Chiu SJ, Lin S, Yang S, Chang WC. STIM1 overexpression promotes colorectal cancer progression, cell motility and COX-2 expression. Oncogene 2015;34:4358–4367.
24. Gandhirajan RK, Meng S, Chandramoorthy HC, Mallilankaraman K, Mancarella S, Gao H, Razmpour R, Yang XF, Houser SR, Chen J, Koch WJ, Wang H, Soboloff J, Gill DL, Madesh M. Blockade of NOX2 and STIM1 signaling limits lipopolysaccharide-induced vascular inflammation. J Clin Invest 2013; 123:887–902.
25. Oh-Hora M, Yamashita M, Hogan PG, Sharma S, Lamperti E, Chung W, Prakriya M, Feske S, Rao A. Dual functions for the endoplasmic reticulum calcium sensors STIM1 and STIM2 in T cell activation and tolerance. Nat Immunol 2008;9:432–443.
26. Ma J, McCarl CA, Khalil S, Lüthy K, Feske S. T-cell-specific deletion of STIM1 and STIM2 protects mice from EAE by impairing the effector functions of Th1 and Th17 cells. Eur J Immunol 2010;40:3028–3042.
27. Schuhmann MK, Stegner D, Berna-Erro A, Bittner S, Braun A, Kleinschnitz C, Stoll G, Wiendl H, Meuth SG, Nieswandt B. Stromal interaction molecules 1 and 2 are key regulators of autoreactive T cell activation in murine autoimmune central nervous system inflammation. J Immunol 2010;184:1536–1542.
28. Kaufmann U, Kahlfuss S, Yang J, Ivanova E, Koralov SB, Feske S. Calcium signaling controls pathogenic Th17 cell-mediated inflammation by regulating mitochondrial function. Cell Metab 2019;29:1104–1118.e6.
29. Schwarz A, Tutsch E, Ludwig B, Schwarz EC, Stallmach A, Hoth M. Ca2+ signaling in identified T-lymphocytes from human intestinal mucosa. Relation to hyporeactivity, proliferation, and inflammatory bowel disease. J Biol Chem 2004;279:5641–5647.
30. Engstrom JF, Arvanitakis C, Sagawa A, Abdou NI. Secretory immunoglobulin deficiency in a family with inflammatory bowel disease. Gastroenterology 1978; 74:747–751.
31. Hasnain SZ, Tauro S, Das I, Tong H, Chen AC, Jeffery PL, McDonald V, Florin TH, McGuckin MA. IL-10 promotes production of intestinal mucus by suppressing protein misfolding and endoplasmic reticulum stress in goblet cells. Gastroenterology 2013;144:357–368.e9.
32. Herp S, Brugiroux S, Garzetti D, Ring D, Jochum LM, Beutler M, Eberl C, Hussain S, Walter S, Gerlach RG, Ruscheweyh HJ, Huson D, Sellin ME, Slack E, Hanson B, Loy A, Baines JF, Rausch P, Basic M, Bleich A, Berry D, Stecher B. Mucispirillum schaedleri antagonizes salmonella virulence to protect mice against colitis. Cell Host Microbe 2019;25:681–694.e8.
33. Hetz C, Zhang K, Kaufman RJ. Mechanisms, regulation and functions of the unfolded protein response. Nat Rev Mol Cell Biol 2020;21:421–438.
34. Siwecka N, Rozpędek-Kamińska W, Wawrzynkiewicz A, Pytel D, Diehl JA, Majsterek I. The structure, activation and signaling of IRE1 and its role in determining cell fate. Biomedicines 2021;9:156.
35. Bahar E, Kim H, Yoon H. ER Stress-mediated signaling: action potential and Ca(2+) as key players. Int J Mol Sci 2016;17:1558.
36. Lupp C, Robertson ML, Wickham ME, Sekirov I, Champion OL, Gaynor EC, Finlay BB. Host-mediated inflammation disrupts the intestinal microbiota and promotes the overgrowth of Enterobacteriaceae. Cell Host Microbe 2007;2:119–129.
37. Nagalingam NA, Kao JY, Young VB. Microbial ecology of the murine gut associated with the development of dextran sodium sulfate-induced colitis. Inflamm Bowel Dis 2011;17:917–926.
38. Nadeem MS, Kumar V, Al-Abbasi FA, Kamal MA, Anwar F. Risk of colorectal cancer in inflammatory bowel diseases. Semin Cancer Biol 2020;64:51–60.
39. Martens EC, Neumann M, Desai MS. Interactions of commensal and pathogenic microorganisms with the intestinal mucosal barrier. Nat Rev Microbiol 2018;16:457–470.
40. Packey CD, Sartor RB. Commensal bacteria, traditional and opportunistic pathogens, dysbiosis and bacterial killing in inflammatory bowel diseases. Curr Opin Infect Dis 2009;22:292–301.
41. Morgan XC, Tickle TL, Sokol H, Gevers D, Devaney KL, Ward DV, Reyes JA, Shah SA, LeLeiko N, Snapper SB, Bousvaros A, Korzenik J, Sands BE, Xavier RJ, Huttenhower C. Dysfunction of the intestinal microbiome in inflammatory bowel disease and treatment. Genome Biol 2012;13:R79.
42. Xia J, Wang H, Huang H, Sun L, Dong S, Huang N, Shi M, Bin J, Liao Y, Liao W. Elevated Orai1 and STIM1

expressions upregulate MACC1 expression to promote tumor cell proliferation, metabolism, migration, and invasion in human gastric cancer. Cancer Lett 2016; 381:31–40.
43. Patergnani S, Danese A, Bouhamida E, Aguiari G, Previati M, Pinton P, Giorgi C. Various aspects of calcium signaling in the regulation of apoptosis, autophagy, cell proliferation, and cancer. Int J Mol Sci 2020;21:8323.
44. Oakes SA, Papa FR. The role of endoplasmic reticulum stress in human pathology. Ann Rev Pathol 2015; 10:173–194.
45. Strugala V, Dettmar PW, Pearson JP. Thickness and continuity of the adherent colonic mucus barrier in active and quiescent ulcerative colitis and Crohn's disease. Int J Clin Pract 2008;62:762–769.
46. Pullan RD, Thomas GA, Rhodes M, Newcombe RG, Williams GT, Allen A, Rhodes J. Thickness of adherent mucus gel on colonic mucosa in humans and its relevance to colitis. Gut 1994;35:353–359.
47. Nowarski R, Jackson R, Gagliani N, de Zoete MR, Palm NW, Bailis W, Low JS, Harman CC, Graham M, Elinav E, Flavell RA. Epithelial IL-18 equilibrium controls barrier function in colitis. Cell 2015; 163:1444–1456.
48. Okamoto R, Watanabe M. Role of epithelial cells in the pathogenesis and treatment of inflammatory bowel disease. J Gastroenterol 2016;51:11–21.
49. Jakobsson HE, Rodríguez-Piñeiro AM, Schütte A, Ermund A, Boysen P, Bemark M, Sommer F, Bäckhed F, Hansson GC, Johansson ME. The composition of the gut microbiota shapes the colon mucus barrier. EMBO Rep 2015;16:164–177.
50. Ahuja M, Schwartz DM, Tandon M, Son A, Zeng M, Swaim W, Eckhaus M, Hoffman V, Cui Y, Xiao B, Worley PF, Muallem S. Orai1-mediated antimicrobial secretion from pancreatic acini shapes the gut microbiome and regulates gut innate immunity. Cell Metab 2017;25:635–646.
51. Lian J, Cuk M, Kahlfuss S, Kozhaya L, Vaeth M, Rieux-Laucat F, Picard C, Benson MJ, Jakovcevic A, Bilic K, Martinac I, Stathopulos P, Kacskovics I, Vraetz T, Speckmann C, Ehl S, Issekutz T, Unutmaz D, Feske S. ORAI1 mutations abolishing store-operated Ca(2+) entry cause anhidrotic ectodermal dysplasia with immunodeficiency. J Allergy Clin Immunol 2018; 142:1297–1310.e11.
52. Pabst O. New concepts in the generation and functions of IgA. Nat Rev Immunol 2012;12:821–832.
53. Bravo R, Parra V, Gatica D, Rodriguez AE, Torrealba N, Paredes F, Wang ZV, Zorzano A, Hill JA, Jaimovich E, Quest AF, Lavandero S. Endoplasmic reticulum and the unfolded protein response: dynamics and metabolic integration. Int Rev Cell Mol Biol 2013; 301:215–290.
54. Ly LD, Xu S, Choi SK, Ha CM, Thoudam T, Cha SK, Wiederkehr A, Wollheim CB, Lee IK, Park KS. Oxidative stress and calcium dysregulation by palmitate in type 2 diabetes. Exp Mol Med 2017;49:e291.
55. Gombedza FC, Shin S, Kanaras YL, Bandyopadhyay BC. Abrogation of store-operated Ca(2+) entry protects against crystal-induced ER stress in human proximal tubular cells. Cell Death Discovery 2019;5:124.
56. Li B, Xiao L, Wang ZY, Zheng PS. Knockdown of STIM1 inhibits 6-hydroxydopamine-induced oxidative stress through attenuating calcium-dependent ER stress and mitochondrial dysfunction in undifferentiated PC12 cells. Free Radical Res 2014;48:758–768.
57. Zaki MH, Vogel P, Malireddi RK, Body-Malapel M, Anand PK, Bertin J, Green DR, Lamkanfi M, Kanneganti TD. The NOD-like receptor NLRP12 attenuates colon inflammation and tumorigenesis. Cancer Cell 2011;20:649–660.
58. Yi ES, Boland JM, Maleszewski JJ, Roden AC, Oliveira AM, Aubry MC, Erickson-Johnson MR, Caron BL, Li Y, Tang H, Stoddard S, Wampfler J, Kulig K, Yang P. Correlation of IHC and FISH for ALK gene rearrangement in non-small cell lung carcinoma: IHC score algorithm for FISH. J Thorac Oncol 2011;6:459–465.
59. Logue JB, Stedmon CA, Kellerman AM, Nielsen NJ, Andersson AF, Laudon H, Lindström ES, Kritzberg ES. Experimental insights into the importance of aquatic bacterial community composition to the degradation of dissolved organic matter. ISME J 2016;10:533–545.

Received September 29, 2021. Accepted March 24, 2022.

Correspondence
Address correspondence to: Weidong Han, Sir Run Run Shaw Hospital, School of Medicine, Zhejiang University, 3# East Qingchun Road, Hangzhou, Zhejiang 310016, China. e-mail: hanwd@zju.edu.cn; fax: 86-571-86436673.

CRediT Authorship Contributions
Weidong Han (Conceptualization: Equal; Funding acquisition: Lead; Resources: Lead)
Xiaojing Liang (Conceptualization: Equal; Data curation: Lead; Formal analysis: Lead; Investigation: Lead; Writing – original draft: Lead; Writing – review & editing: Equal)
Jiansheng Xie (Conceptualization: Equal; Writing – review & editing: Supporting)
Hao Liu (Investigation: Supporting; Methodology: Supporting)
Rongjie Zhao (Formal analysis: Equal; Investigation: Supporting; Software: Lead)
Wei Zhang (Writing – review & editing: Supporting)
Haidong Wang (Investigation: Supporting)
Hongming Pan (Conceptualization: Supporting; Funding acquisition: Equal)
Yubin Zhou (Conceptualization: Supporting; Writing – review & editing: Supporting)

Conflicts of interest
The authors disclose no conflicts.

Funding
This work was supported by the National Natural Science Foundation of China (81572361 and 81972745), the Ten Thousand Plan Youth Talent Support Program of Zhejiang Province (ZJWR0108009), and the Zhejiang Medical Innovative Discipline Construction Project-2016.

Data Transparency
The experimental data underlying this article are available in the article. The raw sequence data will be shared on reasonable request.